ELSEVIER

Journal of Chromatography A, 877 (2000) 181–215

JOURNAL OF CHROMATOGRAPHY A

www.elsevier.com/locate/chroma

Modeling the velocity field of the electroosmotic flow in charged capillaries and in capillary columns packed with charged particles: interstitial and intraparticle velocities in capillary electrochromatography systems

A.I. Liapis*, B.A. Grimes

Department of Chemical Engineering and Biochemical Processing Institute, University of Missouri-Rolla, Rolla, MO 65409-1230, USA

Received 20 August 1999; received in revised form 31 January 2000; accepted 3 February 2000

Abstract

Mass transfer systems based on electrokinetic phenomena (i.e., capillary electrochromatography (CEC)) have shown practical potential in becoming powerful separation methods for the biotechnology and pharmaceutical industries. A mathematical model has been constructed and solved to describe quantitatively the profiles of the electrostatic potential, pressure, and velocity of the electroosmotic flow (EOF) in charged cylindrical capillaries and in capillary columns packed with charged particles. The results obtained from model simulations (i) provide significant physical insight and understanding with regard to the velocity profile of the EOF in capillary columns packed with charged porous particles which represent systems employed in CEC, (ii) provide the physical explanation for the experimental results which indicate that the velocity of the EOF in capillary columns packed with charged porous particles is a very weak function (it is almost independent) of the diameter of the particles, and (iii) indicate that the intraparticle velocity, $v_{p,i}$, of the EOF can be greater than zero. The intraparticle Peclet number, $Pe_{int\ rap}$, for lysozyme was found to be greater than unity and this intraparticle convective mass transfer mechanism could contribute significantly, if the appropriate chemistry is employed in the mobile liquid phase and in the charged porous particles, in (a) decreasing the intraparticle mass transfer resistance, (b) decreasing the dispersive mass transfer effects, and (c) increasing the intraparticle mass transfer rates so that high column efficiency and resolution can be obtained. Furthermore, the results from model simulations indicate that for a given operationally permissible value of the applied electric potential difference per unit length, E_x, high values for the average velocity of the EOF can be obtained if (1) the zeta potential, ζ_p, at the surface of the particles packed in the column has a large negative magnitude, (2) the value of the viscosity, μ, of the mobile liquid phase is low, (3) the magnitude of the dielectric constant, ε, of the mobile liquid phase is reasonably large, and (4) the combination of the values of the concentration, C_∞, of the electrolyte and of the dielectric constant, ε, provide a thin double layer. The theoretical results for the velocity of the EOF obtained from the solution of the model presented in this work were compared with the experimental values of the velocity of the EOF obtained from a fused-silica column packed with charged porous silica C_8 particles. Systems with four different particle diameters and three different concentrations of the electrolyte were considered, and the magnitude of the electric field was varied widely. The agreement between theory and experiment was found to be good.

*Corresponding author. Tel.: +1-573-341-4416; fax: +1-573-341-2071.

0021-9673/00/$ – see front matter
PII: S0021-9673(00)00185-0

Keywords: Electroosmotic flow; Charged porous particles; Electrochromatography; Intraparticle electroosmotic flow; Intraparticle convective flow; Intraparticle Peclet number; Capillary columns

1. Introduction

In high-performance liquid chromatography (HPLC) a liquid is driven through a packed bed by the application of a hydrostatic pressure, while in capillary electrochromatography (CEC) a potential difference (an electric field) across the length of the column is used to drive the mobile liquid phase through a packed bed by electroosmotic flow (EOF) [1–9]. The method of CEC uses packed fused-silica capillaries and modified capillary electrophoresis (CE) equipment, and therefore, one could consider that CEC is a hybrid separation method of CE and Micro-HPLC [7,8]. The fused-silica capillaries have inside diameters of 50–100 μm and are packed with HPLC stationary phases. The motion of the liquid under electroosmotic flow (EOF) arises in the electrical double layer at the liquid solid interface. The EOF originates within the electrical double layer which exists at surfaces such as those of silica and octadecylsilica that bear fixed negative charges while the solution in contact with such surfaces contains an excess of positively charged ions. A charged sheath is formed around a core of uncharged liquid by this excess positive charge which is located very close to the surface [5], and shear develops within the sheath when an electric field is applied across the length of the fused-silica capillary. The developed shear moves the charged sheath and the core of uncharged liquid towards the negative electrode. In CEC, the electrolyte that follows the solute(s) of interest as it (they) migrates along the column, is the same as the electrolyte that precedes it.

Experimental results from CEC and HPLC systems [7,8] indicate that CEC offers the following advantages when compared to HPLC: (i) higher column efficiency in CEC than HPLC due to the flow profile of EOF in CEC [5,7], and (ii) there is no column pressure drop limitation in CEC (CEC does not need any pump to maintain a hydraulic flow since the movement of liquid in CEC occurs by EOF) and, thus, micron and submicron size particles can be used [8] as packing materials in CEC and these small size particles provide smaller mass transfer resistance and higher column efficiency. Furthermore, it appears that CEC could have the potential to be implemented into miniaturized systems (K.K. Unger, private communication, 1998) of high throughput, resolution, speed, sensitivity, and precision; these miniaturized systems could allow one in the pharmaceutical and chemical industries to analyze more than ten thousand compounds out of complex natural or synthetic mixtures per day at a concentration level of femtomole per liter and lower.

In order to evaluate and exploit properly the potential of CEC, one would have to have a scientific understanding of the flow profile of EOF in the interstitial channels of bulk flow in packed beds as well as in the intraparticle pores of the porous chromatographic particles used in CEC. The theoretical modeling of the electrokinetic phenomena underlying EOF in packed beds employing nonporous or porous particles could guide the CEC experiments in regions of the experimental space that could lead to novel experimental designs and could provide the mechanistic approach necessary for the understanding of the fundamentals of the physicochemical basis of CEC. A quantitative model that could describe accurately the transport phenomena in CEC systems, could be employed in the design, optimization, and control of such separation processes. Rathore and Horvath [9] in their review paper on the modeling of EOF, conclude that there has not yet been established a solid theoretical understanding of the flow field of EOF in CEC. They strongly indicate that the construction and solution of a mathematical model that could properly describe the electrokinetic phenomena underlying EOF in packed beds, could have the potential to develop CEC into a powerful separation process.

In this work, a mathematical model is constructed and numerically solved in order to obtain the flow field of EOF as well as the radial profiles of the electrical potential and of the pressure in charged cylindrical capillaries and in capillary columns packed with particles having charged surfaces.

2. Mathematical formulation

In CEC, a charged cylindrical capillary of length L and radius R is considered to be packed with charged particles and each particle bears its own electrical double layer. The cylindrical capillary connects two containers having identical solutions of a single electrolyte and the surface of the inner wall of the cylindrical capillary as well as the surface of the particles (external surface if the particles are nonporous; external and internal surfaces if the particles are porous) bear fixed negative charges while the solution in contact with the surfaces contains an excess of positively charged ions. The interstitial channels of bulk flow by EOF are provided by the interstitial voids between the spherical particles and may be considered as being tortuous charged cylindrical capillaries, because the particles must be tightly packed to produce high efficiency and stability of the packed bed. The mean size of the interstitial voids in a column packed with spheres has been shown by a touching sphere model [10,11] and by pore network modeling [12,13] to be about 25–40% of the particle's size. Furthermore, EOF could occur in the pores of the particles if the pore size distribution and pore connectivity of the porous structure of the charged particles are such that intraparticle convective flow [12–18] due to EOF becomes possible. Thus, it is very important for one to have an accurate quantitative model that could describe the flow field of EOF as well as the radial profiles of the electrical potential and of the pressure in charged cylindrical capillaries, since the interstitial channels of bulk flow in CEC and the pores of the charged porous particles packed in a capillary column may be considered as being tortuous charged cylindrical capillaries. In the following sections mathematical models for EOF in charged cylindrical capillaries and in capillary columns packed with particles having charged surfaces are presented.

2.1. Mathematical model for EOF in a charged cylindrical capillary

The continuity, momentum balance, and Poisson equations of a Newtonian liquid at steady-state conditions and low Reynolds numbers are given by the following expressions:

$$\nabla \cdot \rho \mathbf{v} = 0 \tag{1}$$

$$\nabla \cdot (\mu \nabla \mathbf{v}) = \nabla P + \rho_{cd} \nabla \Psi - \frac{1}{8\pi}\left(\rho \frac{\partial \varepsilon}{\partial \rho}\right)\nabla(\nabla\Psi)^2 + \frac{1}{8\pi}(\nabla\Psi)^2 \nabla\varepsilon + \rho \mathbf{g} \tag{2}$$

$$\nabla \cdot (\varepsilon \nabla \Psi) = -4\pi\rho_{cd} \tag{3}$$

In Eqs. (1)–(3), μ is the viscosity of the Newtonian liquid which may change at high electric fields [19], $\mathbf{v}$ is the velocity vector of the liquid, P is the pressure, ρ_{cd} is the liquid space charge density, ε represents the dielectric constant of the liquid, ρ is the density of the liquid, Ψ represents the total electrical potential, and $\mathbf{g}$ denotes the gravitational force per unit mass. The Poisson equation (Eq. (3)) can be incorporated into Eq. 2 (the momentum balance equation) to eliminate ρ_{cd}. In Eq. (2), the third term in the right-hand-side represents the contribution of electrostriction [20] and enhances the stress normal to charged interfaces as it has been shown by Babchin [21]. At very large electric fields [6,20,22,23] a polarization effect is encountered and is represented by the fourth term in the right-hand-side of Eq. (2). If the dielectric constant, ε, of the liquid is approximately independent of space, then the polarization effect may be neglected. Furthermore, if the dielectric constant, ε, is independent of the density of the liquid, then the contribution of electrostriction would be negligible.

There is net flow only along the axial direction, x, of the cylindrical capillary and the velocity components v_r and v_θ along the radial, r, and angular, θ, directions, respectively, are taken to be equal to zero. Thus, the velocity component v_x along the axial direction, x, is nonzero, and, since for a constant density Newtonian liquid Eq. (1) gives $\partial v_x / \partial x = 0$, it is considered that v_x is a function only of the radial direction r ($v_x = v_x(r)$). In Eq. (2), the dielectric constant, ε, is taken to be independent of space and of the density of the liquid, and the viscosity, μ, of the Newtonian liquid is considered to be constant because in this study the electric fields employed will not be very large and will have magnitudes that have been used in practice [8,9,24]. Then by neglecting the inertia term in Eq. (2) the following expressions for the axial (Eq. (4)) and radial (Eq. (5)) com-

ponents of the momentum balance equation are obtained:

$$\frac{d^2 v_x}{dr^2} + \left(\frac{1}{r}\right)\left(\frac{dv_x}{dr}\right) = \left(\frac{1}{\mu}\right)\left(\frac{\partial P}{\partial x}\right) + \rho_{cd}\left(\frac{1}{\mu}\right)\left(\frac{\partial \Psi}{\partial x}\right) \quad (4)$$

$$0 = \frac{\partial P}{\partial r} + \rho_{cd}\left(\frac{\partial \Psi}{\partial r}\right) \quad (5)$$

If there is no applied pressure difference across (along the axial direction x) the charged cylindrical capillary, then $\partial P/\partial x = 0$ in Eq. (4); in Eq. (4), the term $\partial P/\partial x$ is taken to be equal to zero because currently in CEC systems no pressure difference is applied across the capillary column.

The total potential Ψ is decomposed into an electrostatic contribution $\Phi(r)$ that is due to the double layer and an applied contribution $\Gamma(x)$ [25] as follows:

$$\Psi = \Phi(r) + \Gamma(x) \quad (6)$$

The continuity equation gives that $\partial v_x/\partial x = 0$ while the principle of conservation of charge indicates that $\partial i_x/\partial x = 0$. Thus, since there is no radial transport, the continuity equation and the expression for the conservation of charge require [3,25] that $\partial\Gamma(x)/\partial x$ be a constant. Therefore,

$$\frac{d\Gamma(x)}{dx} = -E_x \quad (7)$$

where E_x represents the applied electric potential difference per unit length along the axial direction, x, of the charged cylindrical capillary.

The expression for the equilibrium diffuse double layer is constructed from the Poisson equation (Eq. (3)) by considering the dielectric constant, ε, to be independent of space and the Boltzmann expression [25]. The Boltzmann relation is derived from the steady-state material balance equations for the cations and the anions by considering equilibrium distribution in the radial direction (this requires that the radius R of the capillary is small compared to its length L, as is the case in practice) which provides the following expression:

$$\frac{\partial C_i}{\partial r} + \frac{ez_i C_i}{kT}\frac{\partial \Psi}{\partial r} = 0, \quad i = +, - \quad (8)$$

In Eq. (8), C_+ denotes the concentration of the cations, C_- represents the concentration of the anions, z_+ is the charge number of the cations, z_- denotes the charge number of the anions, and e is the charge of an electron. By using Eq. (6) and integrating Eq. (8), one obtains the Boltzmann relation:

$$C_+ = C_{+\infty}\exp\left(-\frac{ez_+\Phi}{kT}\right) \quad (9)$$

$$C_- = C_{-\infty}\exp\left(-\frac{ez_-\Phi}{kT}\right) \quad (10)$$

When the Debye length is sufficiently small compared to the capillary radius, the double layer is in contact with an electroneutral core region and $C_{+\infty}$ and $C_{-\infty}$ represent the concentrations of the cations and anions, respectively, in that region. When the double layers overlap, Eqs. (9) and (10) remain valid, but now $C_{+\infty}$ and $C_{-\infty}$ represent fictitious concentrations at large distances from the axis where the potential Φ due to the double layer is zero (in this case, $C_{+\infty}$ and $C_{-\infty}$ denote bulk solution concentrations outside the capillary where $\Phi = 0$). The space charge density, ρ_{cd}, is the sum of the ionic charge concentrations at any point and is given by the expression:

$$\rho_{cd} = N_o e(z_+ C_+ + z_- C_-) \quad (11)$$

where N_o is Avogadro's number (6.023×10^{23} mol^{-1}). By substituting Eqs. (9) and (10) into expression (11) one obtains:

$$\rho_{cd} = N_o e\left[z_+ C_{+\infty}\exp\left(-\frac{ez_+\Phi}{kT}\right) + z_- C_{-\infty}\exp\left(-\frac{ez_-\Phi}{kT}\right)\right] \quad (12)$$

For a symmetric electrolyte $z_+ = -z_- = z$ and $C_{+\infty} = C_{-\infty} = C_\infty$ and, thus, Eq. (12) provides the following expression for the charge density, ρ_{cd}, when the electrolyte is symmetric:

$$\rho_{cd} = -2N_o ezC_\infty\left(\sinh\left(\frac{ez\Phi}{kT}\right)\right) \quad (13)$$

By combining Eqs. (3), (6), and (12) and considering that the dielectric constant, ε, is independent of space, the expression for the equilibrium diffuse double layer is obtained and its form is as follows:

$$\frac{d^2\Phi}{dr^2}+\left(\frac{1}{r}\right)\left(\frac{d\Phi}{dr}\right)= -\frac{4\pi}{\varepsilon}\left[N_o e\left(z_+ C_{+\infty}\exp\left(-\frac{ez_+\Phi}{kT}\right)+z_- C_{-\infty}\exp\left(-\frac{ez_-\Phi}{kT}\right)\right)\right] \quad (14)$$

For a symmetric electrolyte, Eq. (14) takes the form:

$$\frac{d^2\Phi_1}{dr^2}+\left(\frac{1}{r}\right)\left(\frac{d\Phi_1}{dr}\right)=\left(\frac{1}{\lambda^2}\right)\sinh(\Phi_1) \quad (15)$$

where

$$\Phi_1=\frac{ez\Phi}{kT} \quad (16)$$

$$\lambda=\left(\frac{\varepsilon kT}{8\pi N_o e^2 z^2 C_\infty}\right)^{1/2} \quad (17)$$

Eq. (15) is the classical Poisson–Boltzmann expression and the parameter λ is called the Debye length and is often used to represent the characteristic thickness of the double layer.

In this work, systems involving symmetric electrolytes are examined and, thus, Eq. (15) is used in order to obtain the radial distribution of the electrostatic potential Φ that is due to the double layer. The boundary condition of Eq. (15) at the centerline of the capillary is as follows:

$$\text{at } r=0,\ \frac{d\Phi_1}{dr}=0 \quad (18)$$

The principle of conservation of charge requires that the total charge in the capillary liquid is equal in magnitude but opposite in sign to the fixed charge at the capillary wall [3]. By using Eq. (3) and the divergence theorem [26], an integral construction of this constraint with respect to the conservation of charge provides [27] the following boundary condition at the capillary wall for Eq. (15):

$$\text{at } r=R,\ \mathbf{n}\cdot\nabla\Phi_1=\left(\frac{4\pi ze}{\varepsilon kT}\right)\delta \quad (19)$$

In Eq. (19), **n** is the unit normal vector pointing outward from the capillary wall and δ represents the fixed charge density at the capillary wall which is an unspecified parameter. Expression (19) provides the following boundary condition for Eq. (15):

$$\text{at } r=R,\ \frac{d\Phi_1}{dr}=\left(\frac{4\pi ze}{\varepsilon kT}\right)\delta \quad (19a)$$

The zeta potential, ζ_w, at the capillary wall ($\Phi(r=R)=\Phi_w=\zeta_w$) can be measured experimentally [28] and, thus, one could employ the following alternative boundary condition at the capillary wall for Eq. (15):

$$\text{at } r=R,\ \Phi_1=\frac{ez\zeta_w}{kT} \quad (20)$$

After Eq. (15) has been solved by using the boundary conditions given by Eqs. (18) and (20), the gradient of Φ_1 at $r=R$ can be evaluated and then the value of δ could be determined from Eq. (19a). By examining the mathematical structure of Eqs. (15), (16) and (18)–(20), one could observe that since the gradient of the electrostatic potential at the wall of the cylindrical capillary is constant ($(d\Phi/dr)|_{r=R}=(4\pi/\varepsilon)\delta$) because the values of ε and δ are constant, then the value of the zeta potential, $\zeta_w(\Phi|_{r=R}=\zeta_w)$, at the capillary wall would increase as the radius R of the capillary decreases; the experimental data of Zhmud [29] confirm this theoretical result. The effect on the velocity, v_x, of the increase in the value of ζ_w when the radius, R, of the capillary is very small and the double layers overlap, could be important. Therefore, it is worth examining and comparing the results for systems where (i) the value of the zeta potential, ζ_w, is taken to be constant for all values of R (the boundary condition given by Eq. (20) is used for Eq. (15)), and (ii) the gradient of the electrostatic potential at the capillary wall is taken to be constant for all values of R (the boundary condition given by Eq. (19a) is used for Eq. (15)). It is very important to be able to determine the value of the fixed charge density, δ, at the capillary wall, since in CEC systems involving the adsorption of adsorbate molecules it is possible that the value of δ could vary with the loading of adsorbate and this could influence the magnitude of the EOF.

By considering Eqs. (6), (7), (13), and (16), as well as that $v_x=v_x(r)$ and $\partial P/\partial x=0$, Eqs. (4) and (5) take the following forms when symmetric electrolytes are used:

$$\frac{d^2v_x}{dr^2}+\left(\frac{1}{r}\right)\left(\frac{dv_x}{dr}\right)= -2N_o ezC_\infty \sinh(\Phi_1)\left(\frac{1}{\mu}\right)(-E_x) \quad (21)$$

$$0=\frac{dP}{dr}-2N_o ezC_\infty \sinh(\Phi_1)\left(\frac{kT}{ez}\right)\left(\frac{d\Phi_1}{dr}\right) \quad (22)$$

The boundary conditions for Eqs. (21) and (22) are as follows:

$$\text{at } r=0, \quad \frac{dv_x}{dr}=0 \quad (23)$$

$$\text{at } r=R, \quad v_x=0 \quad (24)$$

$$\text{at } r=0, \quad P=P_0 \quad (25)$$

The solution of Eq. (22) using Eq. (25) as the boundary condition is given by:

$$P=P_0+2N_oC_\infty kT\left[\cosh(\Phi_1)-\cosh(\Phi_{1,0})\right] \quad (26)$$

where $\Phi_{1,0}$ denotes the value of Φ_1 at $r=0$. From Eq. (26) it can be observed that the pressure at $r=R$ could be substantial if the concentration, C_∞, of the electrolyte has a high magnitude and the value of the electrostatic potential, Φ_1, at $r=R$ is large. Eqs. (15), (18), (19a), (20), (21), (23), and (24) were solved [27] by the method of orthogonal collocation on finite elements [30,31] after defining the dimensionless spatial variable $\xi=r/R$, where ξ varies between zero and one. The numerical solution of these nonlinear ordinary differential equations provides the velocity profile, v_x, of the EOF as well as the profile of the electrostatic potential, Φ_1, along the radial direction of the charged cylindrical capillary. Then the radial profile of the pressure, P, is obtained from Eq. (26). The average velocity, $\langle v_x\rangle$, of the EOF in the charged cylindrical capillary is calculated by summing up all the velocities over a cross-section and then dividing by the cross-sectional area:

$$\langle v_x\rangle=\frac{\int_0^{2\pi}\int_0^R v_x r\,dr\,d\theta}{\pi R^2}=\left(\frac{2}{R^2}\right)\left(\int_0^R v_x r\,dr\right) \quad (27)$$

2.2. Mathematical model for EOF in a charged cylindrical capillary packed with uncharged (neutral) spherical particles

In this system, the EOF is generated at the interface between the electrolyte and the charged wall of the cylindrical capillary while the packed neutral spherical particles of diameter d_p provide the drag force $\mathbf{F}_{drag}$. Knox and Grant [5] and Rathore and Horvath [9] have suggested that the flow in such a system could be considered to be in the form of very thin annuli of liquid where the velocity has a zero value at the surface of the neutral particles. Of course, each annulus is subjected to (i) a force acting along the direction of the EOF from the annulus enveloping it, and (ii) a force acting in the opposite direction of the EOF from the annulus inside it. The total drag force $\mathbf{F}_{drag}$ due to the packed spherical particles could be estimated [32,33] from Eq. (28):

$$\mathbf{F}_{drag}=\gamma\left(\frac{3}{4}\right)\left(\frac{1-\varepsilon_b}{\pi d_p^3}\right)(6\pi\mu d_p v_{xp,un}) \quad (28)$$

where γ is a dimensionless packing parameter that characterizes the structure of the packing formed by the neutral spherical particles packed in the charged cylindrical capillary; the value of γ could be determined experimentally [32,34]. In Eq. (28), the variable $v_{xp,un}$ represents the velocity component of the EOF along the axial direction of the charged capillary packed with uncharged spherical particles. By neglecting the effect of inertia and balancing the net viscous force $\mathbf{F}_{vis}$ on an annulus of unit volume in the absence of neutral particles with the total drag force $\mathbf{F}_{drag}$, expression (29) is obtained:

$$\mu\left[\frac{d^2v_{xp,un}}{dr^2}+\left(\frac{1}{r}\right)\frac{dv_{xp,un}}{dr}\right]=\gamma\left(\frac{3}{4}\right)\left(\frac{1-\varepsilon_b}{\pi d_p^3}\right)(6\pi\mu d_p v_{xp,un}) \quad (29)$$

where the left-hand-side of Eq. (29) represents the expression for $\mathbf{F}_{vis}$. Eq. (29) may be rewritten as:

$$\frac{d^2v_{xp,un}}{dr^2}+\left(\frac{1}{r}\right)\frac{dv_{xp,un}}{dr}=\left(\frac{\kappa}{d_p}\right)^2 v_{xp,un} \quad (30)$$

where

$$\kappa = 3\left(\frac{\gamma(1-\varepsilon_b)}{2}\right)^{1/2} \quad (31)$$

The solution of Eq. (30) which is finite at $r=0$ is given by:

$$v_{xp,un} = BI_0\left(\frac{\kappa}{d_p}r\right) \quad (32)$$

where B is a constant of integration and I_0 is the zero-order modified Bessel function of the first kind. At $r=R$ (R is the radius of the charged capillary) the velocity $v_{xp,un}$ is equal to zero because of the no-slip condition, but this is not a useful boundary condition because it provides the trivial solution. But from the solution of the mathematical model in Section 2.1 it has been found [27] that for a capillary column whose radius R is significantly larger than the Debye length, λ (in fused-silica capillary columns used in practice $R \gg \lambda$), the velocity $v_{xp,un}$ could be approximately equal to the value of the velocity v_x of the unpacked capillary at a position very near the charged wall of the capillary column. Numerous simulations [27] using the mathematical model presented in Section 2.1 have shown that at $r = R - 7\lambda$ the value of v_x can be taken to be approximately equal to the maximum value of v_x ($v_x \cong v_{x,max}$). Therefore, the boundary condition used to establish the value of B in Eq. (32) is as follows:

$$\text{at } r = R - 7\lambda, \quad v_{xp,un} = v_x|_{r=R-7\lambda} \cong v_{x,max} \quad (33)$$

It should be mentioned that the systems considered in practice involve thin double layers and, thus, the distance of 7λ from the charged wall of the capillary column is very small compared with the size of the liquid filled space formed by the particles (used in practice) touching each other and the wall of the capillary; this is even more the case for larger particle diameters. Thus, since systems of thin double layers are considered and $R \gg 7\lambda$, one could consider that $R - 7\lambda \cong R$. By using Eq. (33) in Eq. (32), we obtain the following expression for $v_{xp,un}$:

$$v_{xp,un} = (v_x|_{r=R-7\lambda})\frac{I_0\left(\frac{\kappa}{d_p}r\right)}{I_0\left(\frac{\kappa}{d_p}(R-7\lambda)\right)},$$

$$0 \le r \le R - 7\lambda \cong R \quad (34)$$

where the value of $v_x|_{r=R-7\lambda}$ is obtained from the numerical solution of the mathematical model presented in Section 2.1.

The average velocity $\langle v_{xp,un} \rangle$ of the EOF of the liquid in the capillary column packed with uncharged particles could be determined from the expression:

$$\langle v_{xp,un} \rangle = \left(\frac{\int_0^{2\pi}\int_0^{R-7\lambda} v_{xp,un} r\, dr\, d\theta}{\pi(R-7\lambda)^2}\right)\chi \cong \left(\frac{2}{R^2}\right) \times \left(\int_0^{R-7\lambda} v_{xp,un} r\, dr\right)\chi = \left(\frac{2}{R^2}\right)\left(\frac{v_x|_{r=R-7\lambda}}{I_0\left(\frac{\kappa}{d_p}(R-7\lambda)\right)}\right) \times \left(\int_0^{R-7\lambda} I_0\left(\frac{\kappa}{d_p}r\right) r\, dr\right)\chi \quad (35)$$

where χ represents the conductivity factor which is given by the ratio of the effective conductivity of the packed capillary column filled with the electrolyte solution to the conductivity of the unpacked capillary column filled with the electrolyte solution. The value of χ can be determined experimentally [32,35].

Eqs. (34) and (35) provide quantitative information about the contribution of the capillary inner wall ('wall effect') in CEC as it will become apparent in Section 2.3.

2.3. Mathematical model for EOF in a charged cylindrical capillary packed with charged spherical particles

In CEC systems, the EOF is generated at the wall of the capillary column as well as at the surface of the charged spherical particles (for nonporous particles the external surface is involved, while for porous particles the external surface as well as the surface of the pores (internal surface) is involved). The mean radius, R_{ic}, of the charged interstitial channels of bulk flow by EOF in the charged

capillary column packed with charged spherical particles, takes now the place of the open-capillary radius R (see Section 2.1). The value of R_{ic} is significantly smaller than the value of the radius, r_p ($d_p = 2r_p$), of the charged particles and has been shown [10–13] to be about 25–40% of the size of the radius, r_p, of the particles. The interstitial channels (capillaries) of bulk flow by EOF (i) are connected to each other with a certain capillary connectivity, $n_{T,ic}$ [12,13], (ii) are tortuous, and (iii) have a capillary (channel) size distribution whose mean capillary (channel) radius is equal to the value of R_{ic}. It is also possible that EOF could occur in the pores of charged porous particles and the magnitude of the intraparticle velocity [12–18] would depend on the pore size distribution and pore connectivity, $n_{T,p}$, of the porous structure of the charged particles. The effects of (1) the connectivity, $n_{T,ic}$, of the interstitial channels (capillaries) of bulk flow, (2) the channel size distribution of the interstitial capillaries of bulk flow, (3) the pore connectivity, $n_{T,p}$ of the intraparticle pores, and (4) the pore size distribution of the intraparticle pores, on the velocity of the EOF in a capillary column packed with charged particles could be studied by employing in CEC the pore network modelling theory of Meyers and Liapis [12,13]; this kind of study is beyond the scope of the present work and could be considered in a future investigation.

In this work, as a first approximation, the EOF through the capillary column packed with charged particles is considered as flow through several parallel, tortuous charged cylindrical capillaries (channels) whose radius is equal to R_{ic}, and the zeta potential, ζ_p, of the particles is taken to be equal to the zeta potential, ζ_w, at the wall of the capillary column ($\zeta_w = \zeta_p$). The velocity, $v_{xp,c,w=p}$ (the subscript w = p denotes that $\zeta_w = \zeta_p$), of the EOF, the electrostatic potential, Φ, and the radial pressure, P, along the radial direction in each of such charged interstitial cylindrical capillaries of radius R_{ic} are determined from the numerical solution of the equations of the mathematical model presented in Section 2.1. The average velocity $\langle v_{xp,c}\rangle_{w=p}$ of the EOF of the liquid in the capillary column packed with charged particles could be determined, for the case where $\zeta_w = \zeta_p$, from the expression:

$$\langle v_{xp,c}\rangle_{w=p} = \left(\frac{\int_0^{2\pi}\int_0^{R_{ic}} v_{xp,c,w=p} r\, dr\, d\theta}{\pi R_{ic}^2}\right)\chi = \left(\frac{2}{R_{ic}^2}\right)\left(\int_0^{R_{ic}} v_{xp,c,w=p} r\, dr\right)\chi \quad (36)$$

where again χ represents the conductivity factor and was defined in Section 2.2. The value of χ can be determined experimentally.

When the zeta potential, ζ_w, at the wall of the capillary column is not equal to the zeta potential, ζ_p, of the particles ($\zeta_w \neq \zeta_p$), then the net local velocity, $v_{xp,c,w\neq p}$(the subscript w ≠ p denotes that $\zeta_w \neq \zeta_p$), of the EOF is determined by adding to the velocity $v_{xp,c,w\neq p}$ a term that accounts for the wall effect. This term is obtained by multiplying the right-hand-side of Eq. (34) by $(1-(\zeta_p/\zeta_w))$; in effect, the zeta potential of the wall of the capillary column is being replaced by the excess zeta potential $(\zeta_w - \zeta_p)$ on the wall which is responsible for the 'wall effect.' Thus the expression for $v_{xp,c,w\neq p}$ is given by:

$$v_{xp,c,w\neq p} = v_{xp,c,w=p} + \left(1-\frac{\zeta_p}{\zeta_w}\right)(v_x|_{r=R-7\lambda})\left(\frac{I_0\left(\frac{\kappa}{d_p}r\right)}{I_0\left(\frac{\kappa}{d_p}(R-7\lambda)\right)}\right),$$

$$0 \le r \le R - 7\lambda \cong R \quad (37)$$

where $v_{xp,c,w=p}$ represents the velocity of the EOF in each charged interstitial capillary (channel) of radius R_{ic} when $\zeta_w = \zeta_p$, as discussed above; R denotes the radius of the capillary column and r represents the radial distance in the capillary column. The average velocity $\langle v_{xp,c}\rangle_{w\neq p}$ (the subscript w≠p denotes that $\zeta_w \neq \zeta_p$) of the EOF of the liquid in the capillary column packed with charged particles could be determined, for the case where $\zeta_w \neq \zeta_p$, from Eq. (38):

$$\langle v_{xp,c}\rangle_{w\neq p} = \left[\left(\frac{2}{R_{ic}^2}\right)\left(\int_0^{R_{ic}} v_{xp,c,w=p} r\, dr\right) + \left(1-\frac{\zeta_p}{\zeta_w}\right)\left(\frac{2}{R^2}\right)\left(\frac{v_x|_{r=R-7\lambda}}{I_0\left(\frac{\kappa}{d_p}(R-7\lambda)\right)}\right) \times\left(\int_0^{R-7\lambda} I_0\left(\frac{\kappa}{d_p}r\right) r\, dr\right)\right]\chi \quad (38)$$

where again χ represents the conductivity factor.

The details for the numerical solution of the equations presented in Sections 2.1–2.3 are presented in the report of Grimes [27].

3. Results and discussion

The zeta potential, ζ_p, at the surface of porous silica C_8 particles of diameter 0.5 μm in a mobile phase of 80% acetonitrile–20% 25 m*M* Tris–HCl at pH 8.0 and temperature $T=20$°C, has been measured experimentally (S. Lüdtke, private communication, 1999) and its value was found to be equal to –64.1 mV. The experimental data for this system (S. Lüdtke, private communication, 1999) indicate that the value of ζ_p becomes less negative than -64.1 mV as the value of the pH decreases below 8.0, while the value of ζ_p becomes more negative than -64.1 mV as the value of the pH increases above 8.0. We want to consider the system where $\zeta_p=-64.1$ mV, because the experimental data for the average velocity of the EOF of the above mobile phase in a fused-silica capillary of radius 50 μm packed with porous silica C_8 particles have been measured (K.K. Unger, private communication, 1999), for four different particle diameters ($d_p=0.2$ μm; $d_p=0.5$ μm; $d_p=1.0$ μm; $d_p=3.0$ μm) and for different values of the applied electric potential difference per unit length, E_x. The radius, R_{ic}, of the interstitial channels for bulk flow by EOF in a fused-silica capillary packed with silica C_8 particles is about one-third of the particle radius, r_p (K.K. Unger, private communication, 1999); for example, if the particle radius, r_p, is 0.25 μm ($d_p=0.5$ μm), then the value of R_{ic} is taken to be equal to 0.0833 μm which corresponds to 833.33 Å. For the mobile phase of 80% acetonitrile–20% 25 m*M* Tris–HCl at pH 8 and $T=20$°C, Eqs. (15), (18) and (20) were solved numerically for a charged cylindrical capillary where the value of the zeta potential at the wall, ζ_w, of the capillary was taken to be equal to the zeta potential, ζ_p, of the particles ($\zeta_w=\zeta_p=-64.1$ mV) and the value of the radius, R, of the cylindrical capillary was taken to be equal to the radius, R_{ic}, of the interstitial channels that would be formed if the particles were packed in a capillary column ($R=R_{ic}\cong 0.0833$ μm). The numerical solution of Eqs. (15), (18) and (20) provided the radial distribution of the electrostatic potential, Φ, and then the value of δ was determined from Eq. (19a) and was found to be equal to -7004.94 esu/cm^2. In the following paragraphs, theoretical results obtained from the numerical solution of the mathematical models presented in Sections 2.1.–2.3. are reported, and the experimental data of the velocity of the EOF in packed capillary columns are compared with the theoretical results. For the results of the systems presented in Figs. 1–12, the pH is equal to 8, the temperature is 20°C, the electrolyte is symmetric ($z_+=-z_-=z=1$; $C_{+\infty}=C_{-\infty}=C_\infty$), the value of the dielectric constant, ε, is equal to 47.8 esu^2/dyne per cm^2 (4.2288×10^{-10} C^2/N per m^2), and the values of the density, ρ, and viscosity, μ, of the mobile phase are 836.77 kg/m^3 and 4.99×10^{-4} kg/m per s, respectively. The Debye length, λ, that represents the characteristic length of the double layer is equal to 14.88 Å for the data in Figs. 1–11, while for the results in Fig. 12 the value of λ varies with the concentration, C_∞, of the symmetric electrolyte; $\lambda=33.27$ Å when $C_\infty=5.0$ m*M*, $\lambda=23.53$ Å when $C_\infty=10.0$ m*M*, and $\lambda=14.88$ Å when $C_\infty=25.0$ m*M*.

3.1. Theoretical results for charged capillaries

In Figs. 1–3 the electrostatic potential, Φ, the velocity, v_x, and the pressure difference, $P(r)-P_0$, profiles along the radial direction r of a charged cylindrical capillary are presented for different values of the ratio R/λ and when $E_x=60$ kV/m. The results in Figs. 1a, 2a, and 3a were obtained by keeping the value of the zeta potential, ζ_w, at the

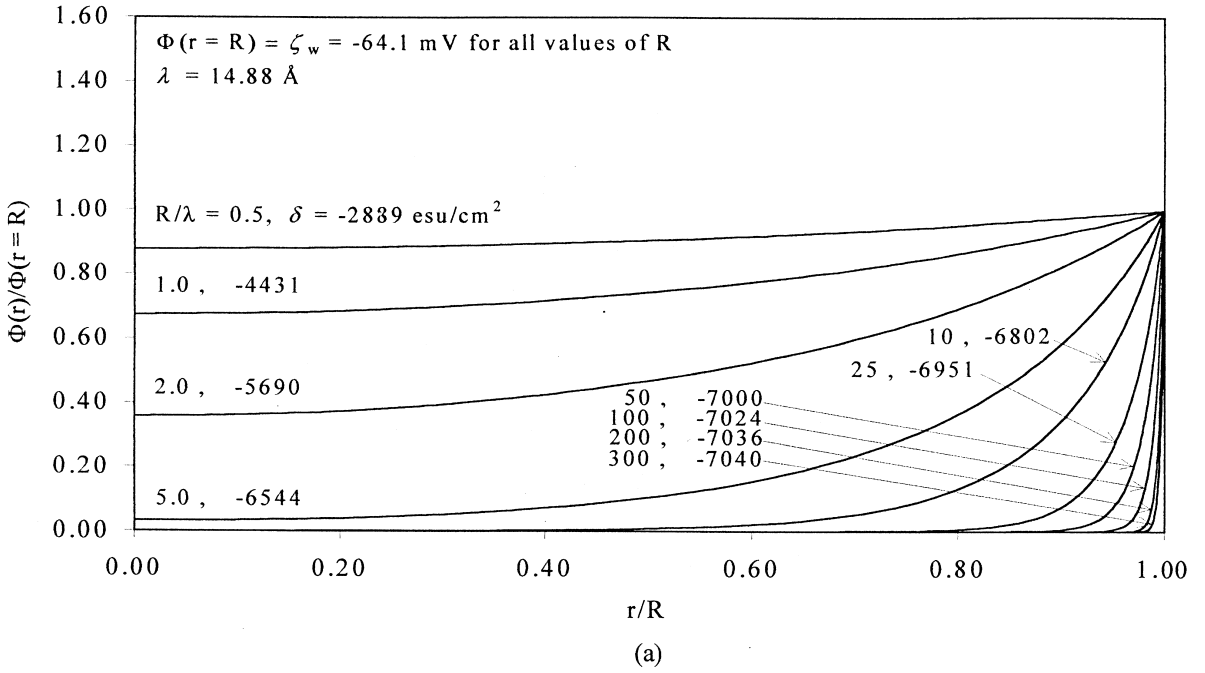

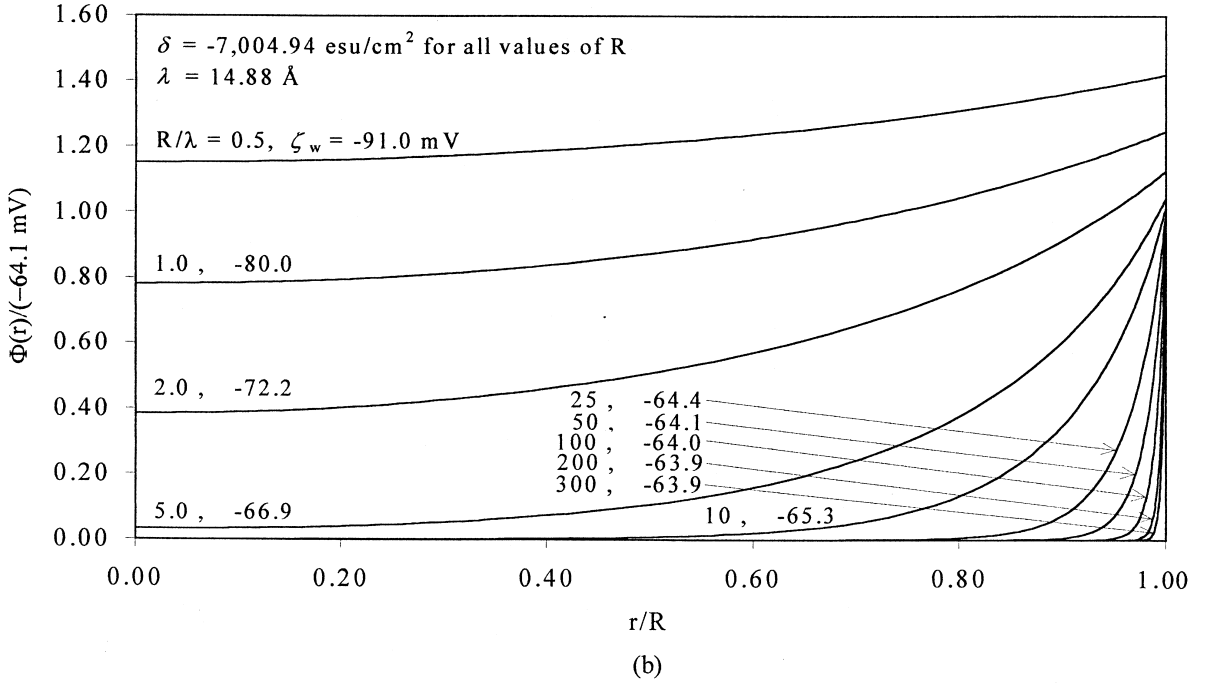

Fig. 1. Electrostatic potential, Φ, profiles at various values of R/λ. The liquid solution is 80% acetonitrile–20% 25 m*M* Tris–HCl at pH 8.0 and $T=20$°C, and the value of the applied electric potential, E_x, is 60 kV/m. (a) $\Phi(r=R)=\zeta_w=-64.1$ mV for all values of R and the reported magnitude of δ for each value of R/λ is determined from Eq. (19a). (b) $\delta=-7004.94$ esu/cm^2 for all values of R and the reported magnitude of ζ_w for each value of R/λ is determined from Eq. (20).

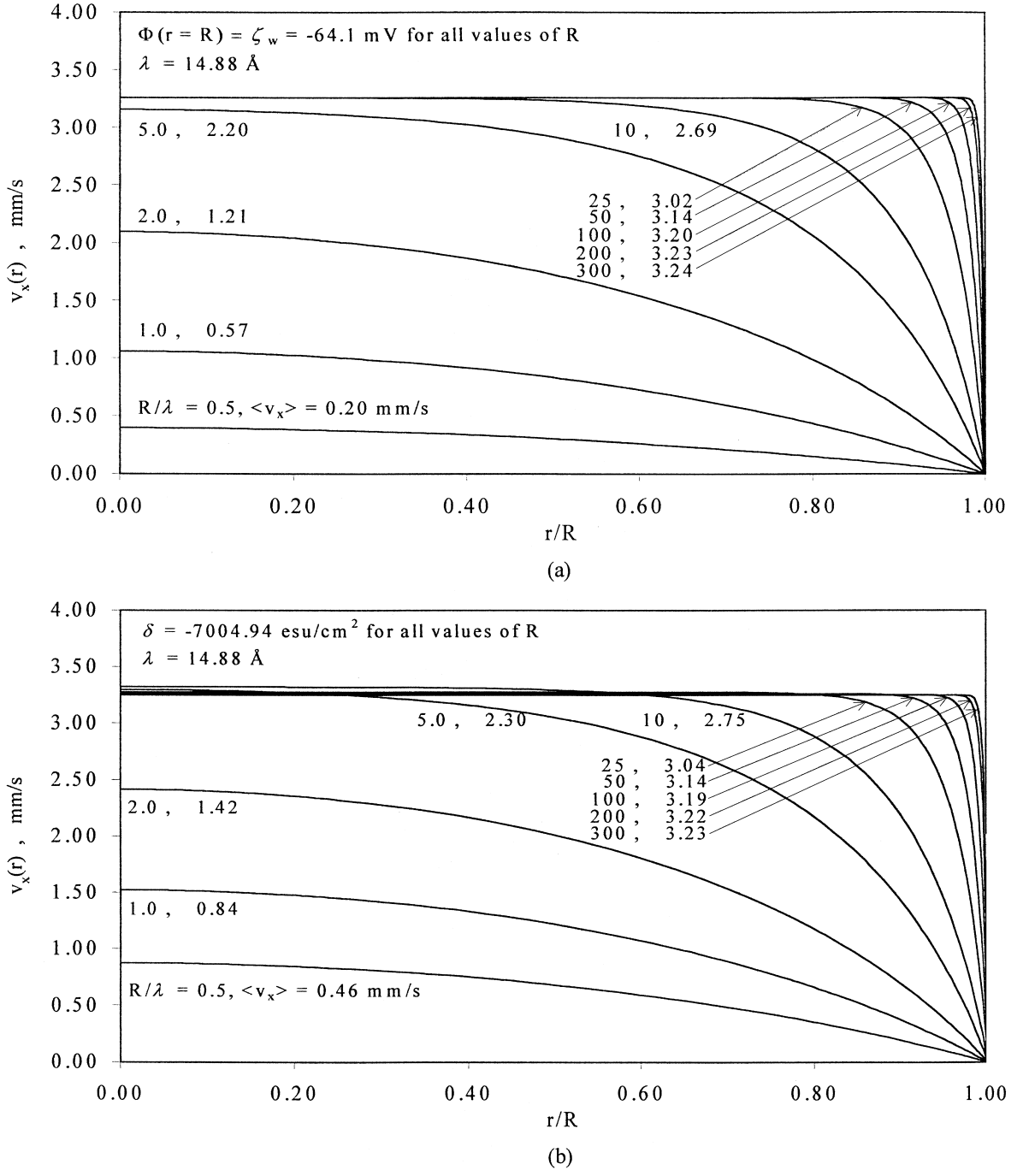

Fig. 2. Velocity, v_x, profiles at various values of R/λ. The liquid solution is 80% acetonitrile–20% 25 m*M* Tris–HCl at pH 8.0 and $T=20°C$, and the value of the applied electric potential, E_x, is 60 kV/m. (a) $\Phi(r=R)=\zeta_w=-64.1$ mV for all values of R and the velocity profiles are determined from the solution of Eqs. (15), (18), (20), (21), (23), and (24). The reported magnitude of the average velocity, $\langle v_x \rangle$, for each value of R/λ is determined from Eq. (27). (b) $\delta=-7004.94$ esu/cm^2 for all values of R and the velocity profiles are determined from the solution of Eqs. (15), (18), (19a), (21), (23), and (24). The reported magnitude of the average velocity, $\langle v_x \rangle$, for each value of R/λ is determined from Eq. (27).

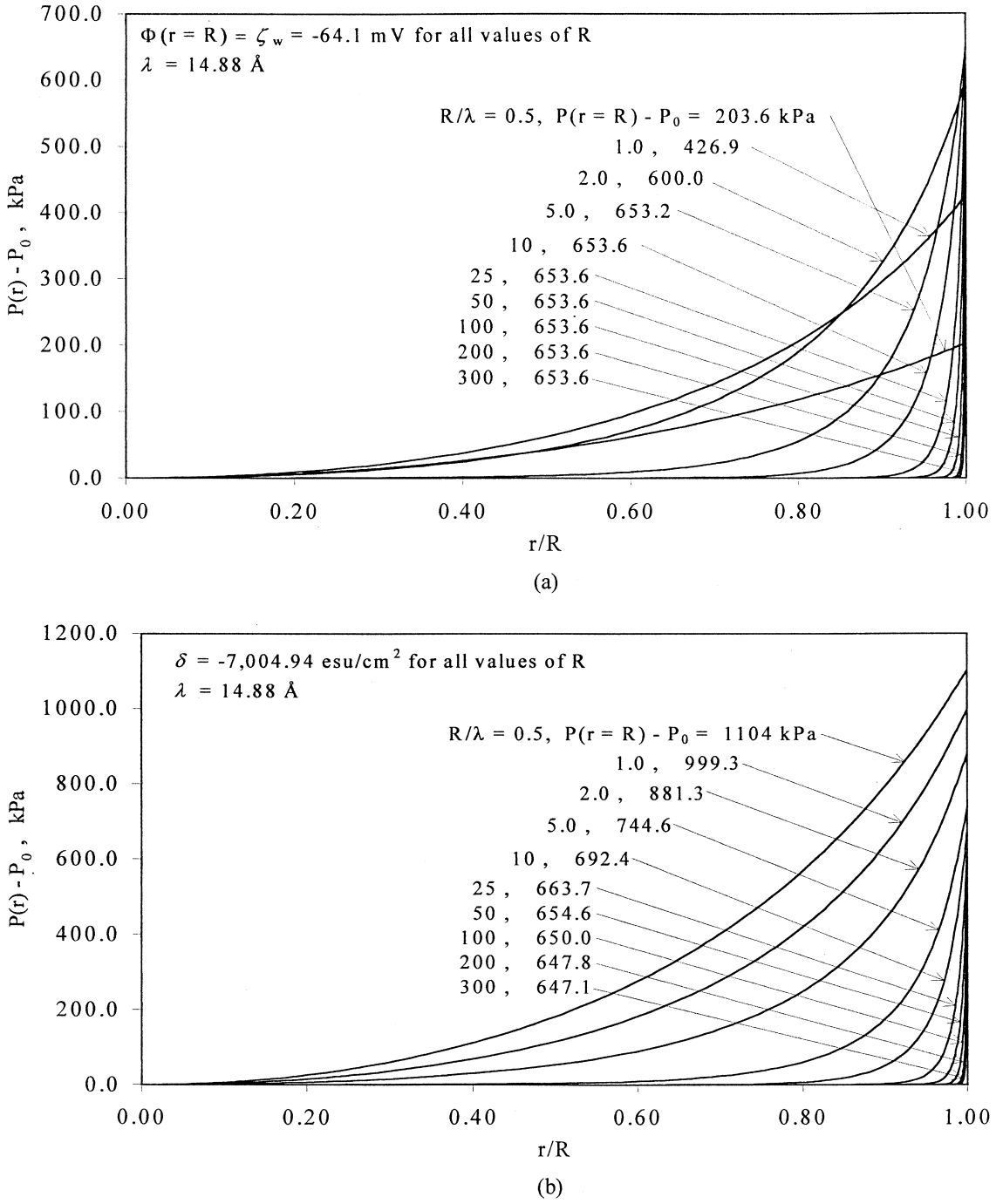

Fig. 3. Pressure difference, $P(r) - P_0$, profiles at various values of R/λ. The liquid solution is 80% acetonitrile–20% 25 m*M* Tris–HCl at pH 8.0 and $T = 20°C$, and the value of the applied electric potential, E_x, is 60 kV/m. (a) $\Phi(r=R) = \zeta_w = -64.1$ mV for all values of R and the pressure difference profiles are determined from the solution of Eqs. (15), (18), (20), and (21)–(26). The reported magnitude of the pressure difference, $P(r = R) - P_0$, between the capillary wall and the centerline for each value of R/λ is determined from Eq. (26). (b) $\delta = -7004.94$ esu/cm^2 for all values of R and the pressure difference profiles are determined from the solution of Eqs. (15), (18), (19a), and (21)–(26). The reported magnitude of the pressure difference, $P(r = R) - P_0$, between the capillary wall and the centerline for each value of R/λ is determined from Eq. (26).

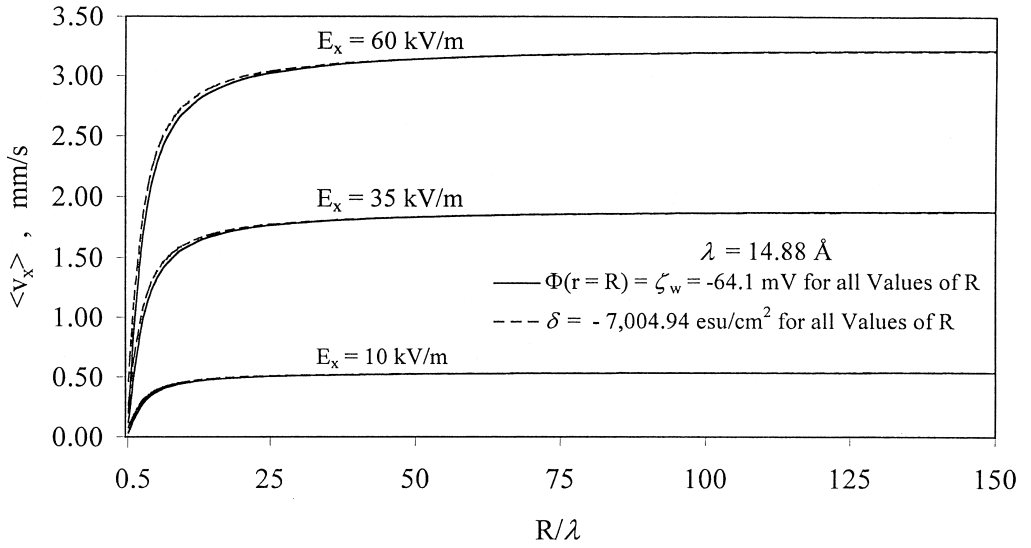

Fig. 4. Average velocity, $\langle v_x \rangle$, versus R/λ for different values of the applied electric potential, E_x. The liquid solution is 80% acetonitrile–20% 25 m*M* Tris–HCl at pH 8.0 and $T = 20$°C.

wall of the charged cylindrical capillary constant (Eq. (20)) and equal to -64.1 mV for all values of R considered and indicated in the figures. The results in Figs. 1b, 2b, and 3b were obtained by keeping the value of δ at the wall of the capillary constant (Eq. (19a)) and equal to -7004.94 esu/cm^2 for all the values of R considered and presented in these figures; in this case, the value of the zeta potential, ζ_w, at the wall of the capillary becomes more negative as the value of the radius R decreases (for

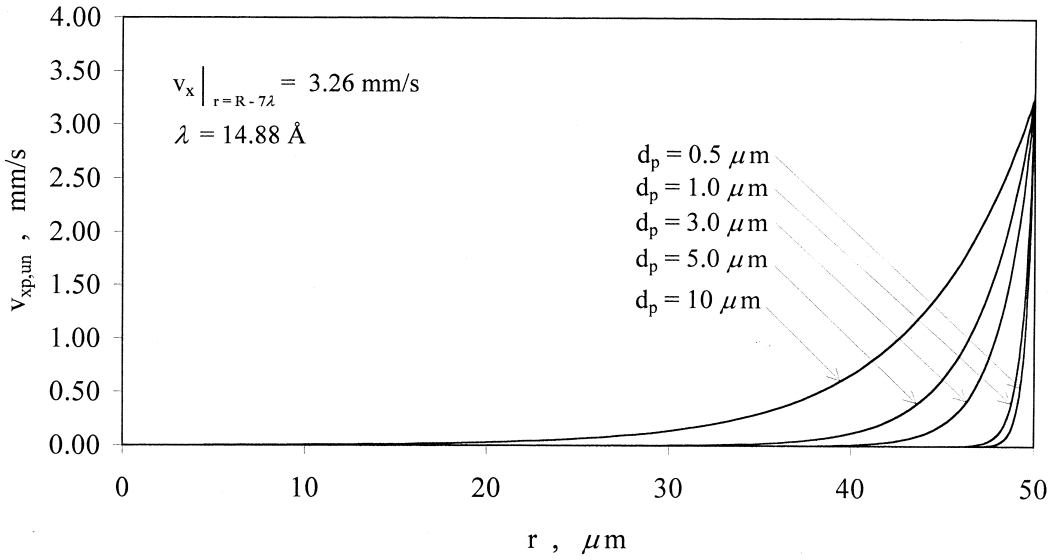

Fig. 5. The effect of the particle diameter, d_p, on the velocity, $v_{xp,un}$, profile in a charged cylindrical capillary packed with uncharged (neutral) particles; $R = 50$ μm, $\Phi(r = R) = \zeta_w = -64.1$ mV, and $E_x = 60$ kV/m. The liquid solution is 80% acetonitrile–20% 25 m*M* Tris–HCl at pH 8.0 and $T = 20$°C.

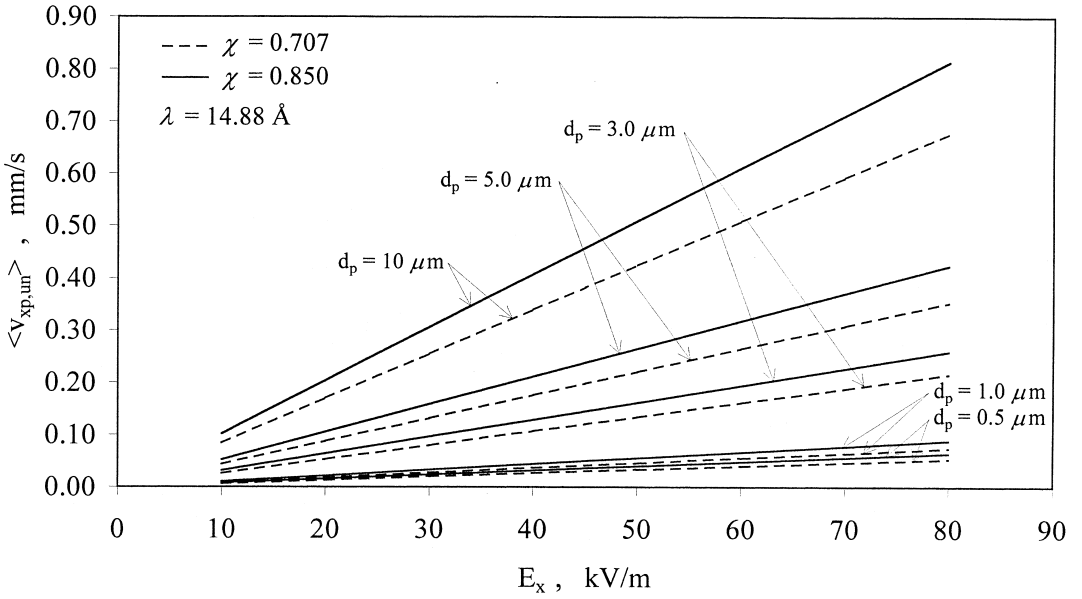

Fig. 6. Average velocity, $\langle v_{xp,un} \rangle$, versus E_x, for different values of the diameter, d_p, of the uncharged (neutral) particles packed in a charged cylindrical capillary of radius $R=50$ μm; two different values of the conductivity factor, χ, are examined and $\Phi(r=R)=\zeta_w=-64.1$ mV. The liquid solution is 80% acetonitrile–20% 25 m*M* Tris–HCl at pH 8.0 and $T=20$°C.

the reason discussed in Section 2.1.), especially when the value of R is such that significant overlap of the double layers in the capillary occurs. In Fig. 1a,b it can be observed that $\Phi(r)=0$ for a significant fraction of the radius when $R/\lambda \geq 10$. For values of $R/\lambda \leq 5.0$, the value of $\Phi(r)$ is nonzero for all values of r and this indicates that the formation of the diffuse double layer is disturbed and overlap of the double layers occurs within such capillaries. In Fig. 1a, the results indicate that when the value of ζ_w is kept constant the value of δ becomes less negative as the radius, R, of the capillary decreases, and the value of δ becomes significantly less negative when R is of the same order of magnitude as λ and disturbed formation of the diffuse double layer as well as overlap of the double layers within the capillary occur. The results in Fig. 1b show that when δ is kept constant the value of ζ_w becomes more negative as the radius, R, of the capillary decreases, and the value of ζ_w becomes significantly more negative when the value of R is small enough that disturbed formation of the diffuse double layer and overlap of the double layers within the capillary occur. In Fig. 2a,b it can be observed that the velocity, v_x, has a plug-flow profile after a certain distance from the wall when the value of R is significantly larger than the value of λ, and this distance from the wall, which indicates the position at which the plug-flow profile starts, decreases as the ratio of R/λ increases; for values of $R/\lambda \geq 50$ it is found that the value of v_x is approximately equal to its plug flow value at a distance 7λ from the wall of the capillary. When R is of the same order of magnitude as λ and disturbed formation of the diffuse double layer as well as overlap of the double layers within the capillary occur, the velocity profile is found to be parabolic for all values of r, as the results in Fig. 2a,b show. Furthermore, when δ is kept constant for all values of R, the results in Fig. 2b indicate that for certain values of R/λ (e.g., $R/\lambda=5.0$) the value of v_x at certain radial positions close to the center of the capillary could have a magnitude which is higher than the magnitude of the plug-flow velocity, but still the average velocity, $\langle v_x \rangle$, in the capillary with the parabolic velocity profile is lower than the average velocity, $\langle v_x \rangle$, obtained in the capillary whose radius, R, is significantly larger than the value of λ and the velocity, v_x, in the capillary has a plug-flow profile for a significant portion of the radius R. The data in Fig.

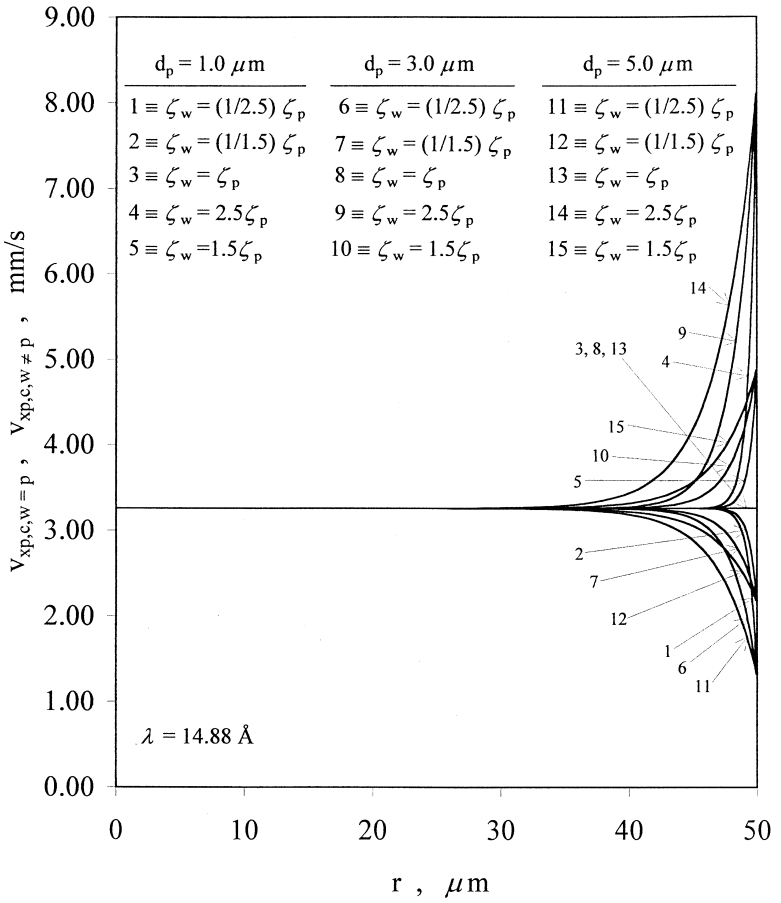

Fig. 7. The 'wall effect' on the velocity, $v_{xp,c,w=p}$ and $v_{xp,c,w\neq p}$, profiles in a charged cylindrical capillary column packed with charged particles for different values of the zeta potential, ζ_w, at the wall and for different particle diameters, d_p; $R=50$ μm, $\zeta_p=-64.1$ mV, $\Phi(r=R)=\zeta_w$ and $E_x=60$ kV/m. The liquid solution is 80% acetonitrile–20% 25 m*M* Tris–HCl at pH 8.0 and $T=20$°C.

2a,b clearly indicate that the average velocity, $\langle v_x \rangle$, is nonzero even at charged cylindrical capillaries having very small values of radius R (e.g., $R \geq 10$ Å) where disturbed formation of the diffuse double layer as well as overlap of the double layers in the capillary occur. This is a very important result because it implies that it is possible for intraparticle convective (EOF) flow to occur in the pores [12–18] of the charged porous particles (e.g., porous silica C_8 particles) used in CEC [7,8,36] (K.K. Unger, private communication, 1998, 1999). The occurrence of intraparticle EOF in the pores of the charged porous particles employed in CEC, could significantly reduce the resistance for mass transfer of adsorbate molecules in such porous media and, thus, substantially increase the capillary column efficiency. The pore network modeling theory of Meyers and Liapis [12,13] could be used to determine the magnitude of the intraparticle EOF in the pores of charged porous particles packed in a capillary column. In Fig. 3a,b the radial profiles of the pressure difference, $P(r) - P_0$, are presented, for different values of R/λ. The results clearly indicate that (i) the pressure at the capillary wall ($P(r=R)$) can be significant, and (ii) the radial length (from the centerline of the capillary) along which $P(r) - P_0 = 0$ increases as the value of the ratio R/λ increases. The results in Fig. 3a indicate that when $\Phi(r=R)=\zeta_w=-64.1$ mV for all values of R, the pressure difference, $P(r=R) - P_0$, between the capillary wall and the centerline

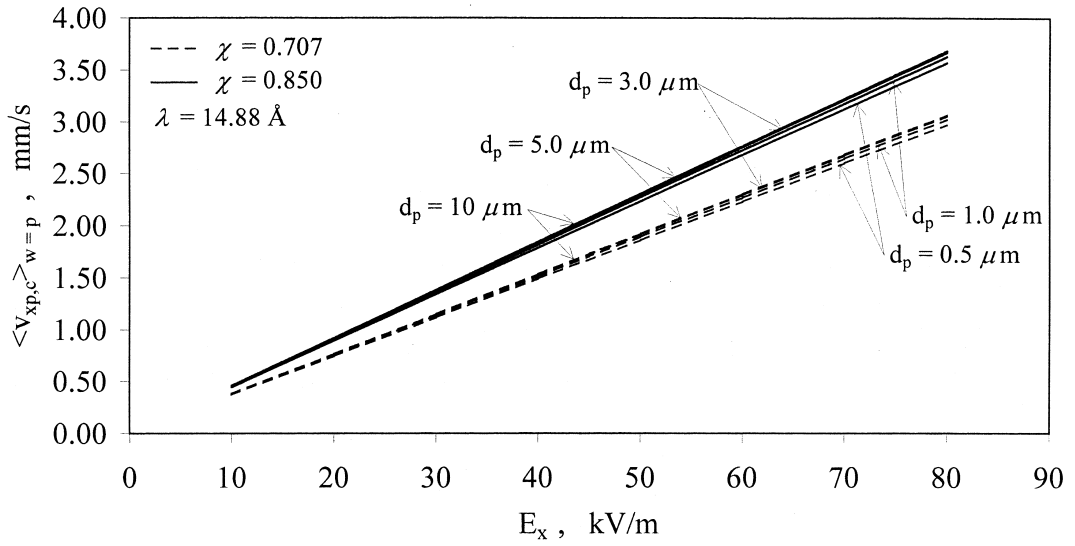

Fig. 8. Average velocity, $\langle v_{xp,c}\rangle_{w=p}$, vs. E_x, for different values of the diameter, d_p, of the charged particles packed in a charged cylindrical capillary of radius $R=50$ μm; two different values of the conductivity factor, χ, are examined and $\Phi(r=R)=\zeta_w=\zeta_p=-64.1$ mV. The liquid solution is 80% acetonitrile–20% 25 m*M* Tris–HCl at pH 8.0 and $T=20$°C.

decreases as the value of the ratio R/λ decreases and the decrease in the value of $P(r=R)-P_0$ is very significant when the radius, R, of the capillary is very small and disturbed formation of the diffuse double layer as well as overlap of the double layers in the capillary occur. In Fig. 3b the data show that when the value of δ is kept constant for all values of R, the pressure difference, $P(r=R)-P_0$, between the capillary wall and the centerline increases as the value of the ratio R/λ becomes less than or equal to 10 because the zeta potential, ζ_w, at the wall of these small capillaries increases significantly as the radius

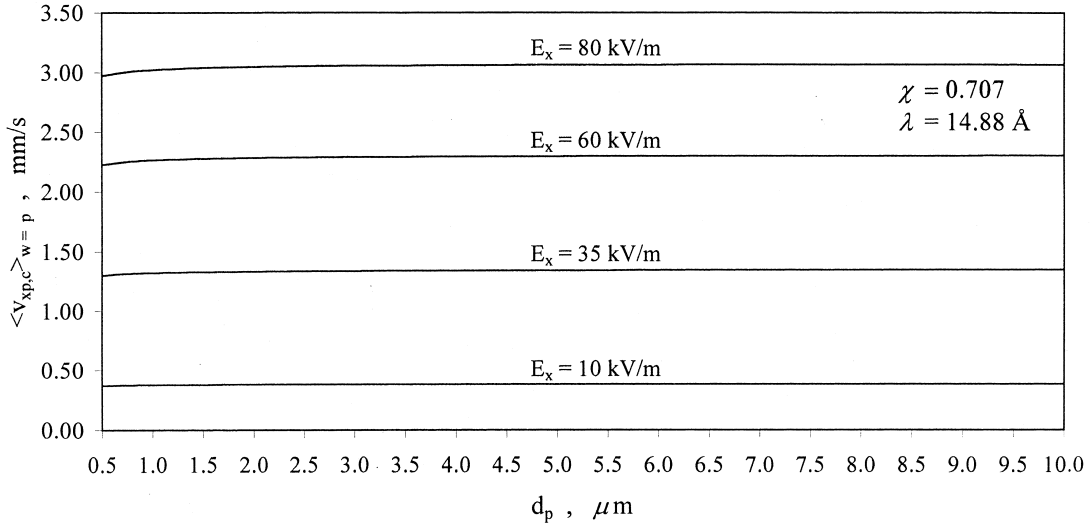

Fig. 9. Average velocity, $\langle v_{xp,c}\rangle_{w=p}$, vs. the particle diameter, d_p, of charged particles with $\zeta_p=\zeta_w$ packed in a charged cylindrical capillary of radius $R=50$ μm for different values of E_x; $\chi=0.707$ and $\Phi(r=R)=\zeta_w=\zeta_p=-64.1$ mV. The liquid solution is 80% acetonitrile–20% 25 m*M* Tris–HCl at pH 8.0 and $T=20$°C.

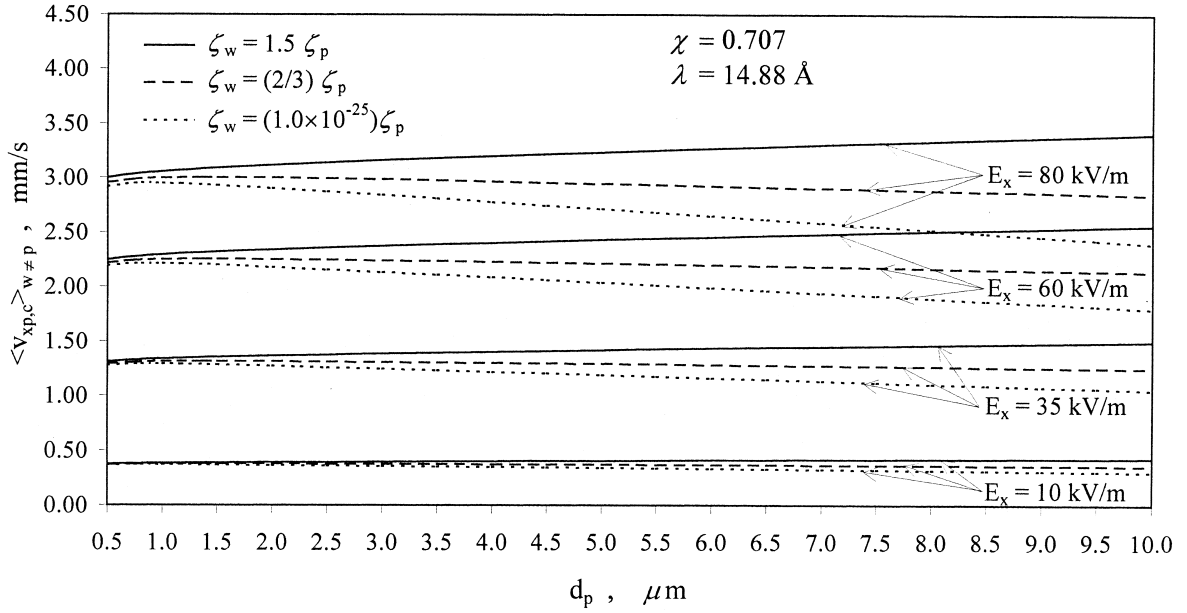

Fig. 10. Average velocity, $\langle v_{xp,c}\rangle_{w\neq p}$, vs. the particle diameter, d_p, of charged particles with $\zeta_p \neq \zeta_w$ packed in a charged cylindrical capillary of radius $R=50$ μm for different values of E_x; $\chi=0.707$, $\zeta_p=-64.1$ mV and $\Phi(r=R)=\zeta_w$. The liquid solution is 80% acetonitrile–20% 25 m*M* Tris–HCl at pH 8.0 and $T=20$°C.

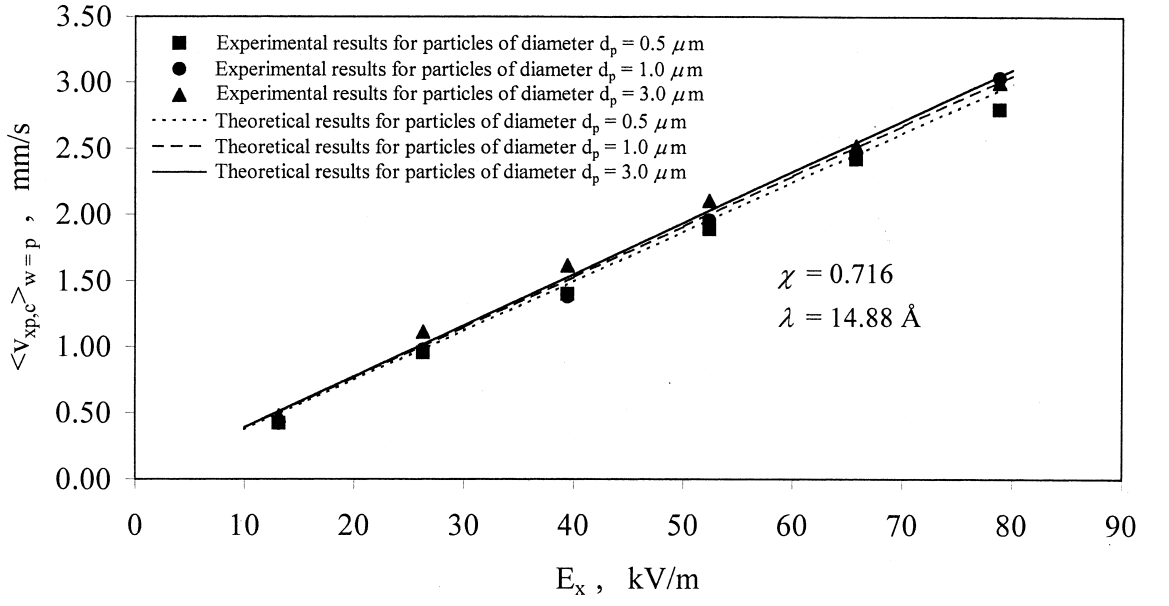

Fig. 11. Comparison of the theoretical results with the experimental data of the average velocity, $\langle v_{xp,c}\rangle_{w=p}$, of the EOF in a fused-silica capillary of radius $R=50$ μm packed with porous silica C_8 particles; $\zeta_w=\zeta_p=-64.1$ mV and $\Phi(r=R)=\zeta_w$. The liquid solution is 80% acetonitrile–20% 25 m*M* Tris–HCl at pH 8.0 and $T=20$°C.

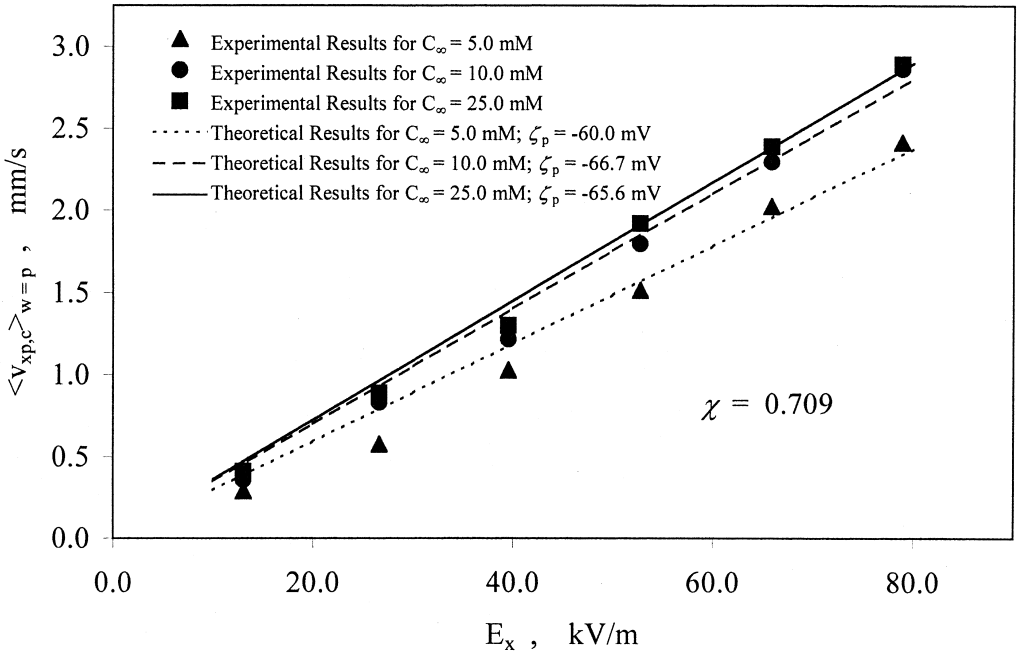

Fig. 12. Comparison of the theoretical results with the experimental data of the average velocity, $\langle v_{xp,c}\rangle_{w=p}$, of the EOF in a fused-silica capillary of radius $R=50$ μm packed with porous silica C_8 particles of diameter $d_p=0.2$ μm, for three different values of the concentration, C_∞, of the electrolyte; $\zeta_w=\zeta_p$ and $\Phi(r=R)=\zeta_w$. The liquid solution is 80% acetonitrile–20% C_∞ m*M* Tris–HCl (80:20, v/v) at pH 8.0 and $T=20$°C.

R of the capillary decreases and becomes comparable to the value of the characteristic length, λ, of the double layer. For values of $R/\lambda>10$ the results in Fig. 3b indicate that the pressure difference, $P(r=R)-P_0$, between the wall of the capillary and the centerline decreases, and for values of $R/\lambda\geq 50$ the values of the pressure difference, $P(r=R)-P_0$, between the capillary wall and the centerline are insignificantly different than the values of the pressure difference, $P(r=R)-P_0$, presented in Fig. 3a for magnitudes of the ratio R/λ greater than or equal to 50.

In Fig. 4 the average velocity, $\langle v_x\rangle$, in a charged cylindrical capillary versus R/λ is presented for different values of E_x. It can be observed, as expected, that the value of $\langle v_x\rangle$ increases significantly, for a given value of R/λ, as the magnitude of E_x is increased. Furthermore, as the value of E_x increases the value of the ratio R/λ at which the average velocity $\langle v_x\rangle$ attains its maximum value, is slightly increased. By comparing, for a given value of E_x, the results provided by the solid ($\zeta_w=-64.1$ mV for all values of R) and dashed ($\delta=-7004.94$ esu/cm^2 for all values of R) curves, one can observe that the values of $\langle v_x\rangle$ obtained when (a) ζ_w is kept constant for all values of R or (b) δ is kept constant for all values of R, are insignificantly different for values of R/λ greater than or equal to 10.

The results in Figs. 1–3 indicate that the values of Φ, v_x, and $P(r)-P_0$ are being influenced by the condition considered at the capillary wall with respect to the values of ζ_w and δ. The data in Figs. 1–3 indicate that the differences in the values of Φ, v_x, and $P(r)-P_0$ obtained (a) by keeping the value of ζ_w constant for all values of R or (b) by keeping the value of δ constant for all values of R, decrease significantly as R/λ increases and become insignificant at large values of R/λ ($R/\lambda\geq 50$). The largest differences occur when the value of R is of the same order of magnitude as the value of λ (small values of R/λ) and disturbed formation of the diffuse double layer as well as overlap of the double layers in the capillary occur. In practical CEC systems the radii of the large intraparticle pores of the charged porous

particles, the radii of the interstitial channels for bulk flow by EOF in the packed capillary column, and the radius of the capillary column are larger than the value of λ by more than one to four orders of magnitude, and therefore, the differences in the results for Φ, v_x, and $P(r)-P_0$ obtained by using either a constant value of ζ_w or a constant value of δ at the wall of such capillaries, would be insignificant. In practice, one can measure without undue difficulty the zeta potential at the wall of the capillary column and at the surface of the particles and, thus, these experimental values could be used to represent, respectively, the values of Φ (Eq. (20)) at the wall of the capillary column and at the wall of the interstitial channels of bulk flow formed by the packed particles in the capillary column. The respective values of δ at the wall of the capillary column and at the wall of the interstitial channels for bulk flow could then be determined from Eq. (19a) and the respective profiles of Φ in the capillary column and the interstitial channels of bulk flow. Then if the pore size distribution of the porous structure of the particles packed in the capillary column has been determined [12,13], the value of δ at the wall of the interstitial channels of bulk flow could be taken to represent, as a first approximation, the magnitude of δ at the wall of the intraparticle pores of different radii and, thus, the velocity profile and the average velocity in an intraparticle pore of a given radius could be estimated; this procedure, although it may be possible that the value of δ may not be the same for the intraparticle pores of varying radii, could provide a useful insight about the possibility of intraparticle EOF and the information obtained with respect to the average velocity of the liquid in the intraparticle pores of different radii could be used in a pore network model for the porous particles to estimate the magnitude of the velocity of the intraparticle EOF in the porous particles. Most importantly, the results in Fig. 4 indicate that the average velocity $\langle v_x \rangle$ obtained (a) by keeping ζ_w constant for all values of R or (b) by keeping δ constant for all values of R, have insignificant differences for magnitudes of $R/\lambda \geq 10$. Since from an engineering perspective one would have more interest in obtaining accurate estimates for the values of the average velocities in the interstitial channels of bulk flow as well as in the pores of charged particles than to determine very accurately the profiles of Φ, v_x, and $P(r)-P_0$ in these capillaries, it is gratifying that the accurate estimation of the average velocity, $\langle v_x \rangle$, becomes essentially independent of the approach of using constant value of ζ_w for all values of R or constant value of δ for all values of R when the magnitude of the ratio R/λ is greater than or equal to 10. It is important to note that the ratio $R/\lambda \geq 10$ for the average velocity, $\langle v_x \rangle$, is more inclusive with respect to capillaries of smaller radii than the ratio $R/\lambda \geq 50$ that was found to provide accurate estimates for the radial profiles of Φ, v_x, and $P(r)-P_0$ which (the profiles) are essentially independent of using either constant ζ_w for all values of R or constant δ for all values of R.

3.2. Theoretical results for capillary columns packed with uncharged (neutral) particles

In Fig. 5, the velocity profile along the radial direction of a charged cylindrical capillary packed with neutral (uncharged) particles is presented (Eq. (34)), for different values of the diameter, d_p, of the particles; the radius, R, of the capillary is 50 μm, $E_x = 60$ kV/m, the value of the zeta potential, ζ_w, at the wall of the capillary is equal to -64.1 mV, the porosity ε_b was taken to be equal to 0.35 and the value of γ (Eq. (28)) was taken to be equal to unity [32,34,35]. As expected, the fraction of the radial length from the wall of the capillary along which the velocity $v_{xp,un}$ is nonzero, increases as the particle diameter, d_p, increases since the magnitude of the drag force, $\mathbf{F}_{drag}$ (Eq. (28)), decreases with increasing particle diameter. Furthermore, for a given position r along the radius where the value of $v_{xp,un}$ is nonzero for all particle diameters, the magnitude of the velocity $v_{xp,un}$ increases as the particle diameter increases. In Fig. 6, the average velocity $\langle v_{xp,un} \rangle$ (Eq. (35)) of the EOF of the liquid in the charged capillary column packed with neutral particles is presented, for different particle diameters, different values of the applied electric potential, E_x, and for two different values of the conductivity factor χ; the values of R, ζ_w, ε_b, and γ are equal to those used to obtain the results in Fig. 5. The value of $\chi = 0.707$ is obtained by setting $\chi = 1/1.414$ where the number 1.414 has been suggested [35] to represent approximately the value of the tortuosity factor, τ, for

columns packed with impermeable spherical particles. If the value of the connectivity parameter, $n_{T,ic}$, of the interstitial channels of bulk flow in the packed capillary column [12,13] has a very high value and the particles are permeable, then the value of χ could be higher than 0.707; thus, the value of $\chi = 0.850$ was arbitrarily selected to represent such a hypothetical packed capillary column. The results in Fig. 6 clearly indicate that the value of the average velocity $\langle v_{xp,un} \rangle$ of the EOF in a charged capillary column packed with neutral particles, increases with increasing values of E_x, d_p, and χ. The results also show that the increase in the value of $\langle v_{xp,un} \rangle$ as E_x increases, is linear. Furthermore, the results indicate that for particles of diameter, d_p, in the range of 0.5–1.0 μm, the values of $\langle v_{xp,un} \rangle$ differ from each other by insignificant amounts when the value of E_x is between 10 and 30 kV/m, while at values of E_x higher than 30 kV/m there are some very small differences in the values of $\langle v_{xp,un} \rangle$.

3.3. Theoretical results for capillary columns packed with charged particles

In Fig. 7 the radial profile of the velocity in a charged capillary column packed with charged particles is presented for different particle diameters and when the value of the zeta potential, ζ_w, at the wall of the capillary is larger than or equal to or smaller than the value of the zeta potential, ζ_p, at the surface of the particles; the value of E_x is equal to 60 kV/m and the radius of the capillary is 50 μm. The results show that (a) the effect of the value of the particle diameter, d_p, on the magnitude of the velocity increases, as the particle diameter, d_p, increases and the magnitude of the difference $(\zeta_w - \zeta_p)$ increases for the case where $\zeta_w > \zeta_p$, and (b) the effect of the magnitude of d_p on the value of the velocity increases, as the particle diameter, d_p, increases and the magnitude of the difference $(\zeta_p - \zeta_w)$ increases for the case where $\zeta_p > \zeta_w$. Furthermore, the enhancement occurring in the value of the velocity, $v_{xp,c,w\neq p}$, close to the capillary wall when ζ_w is greater than ζ_p by a factor σ ($\sigma = 1.5$, 2.5 in Fig. 7), is significantly larger than the retardation that occurs in the value of $v_{xp,c,w\neq p}$ close to the capillary wall when ζ_p is larger than ζ_w by the same factor σ. This difference in the magnitudes of the enhancement and retardation of the velocity, $v_{xp,c,w\neq p}$, is due to the fact that when $\zeta_w > \zeta_p$ there is a synergism between the velocity field due to the zeta potential of the wall and the velocity fields in the interstitial channels for bulk flow located close to the wall, while when $\zeta_p > \zeta_w$ the slower velocity field due to the zeta potential of the wall hinders the velocity fields in the interstitial channels for bulk flow located close to the wall. It is also worth noting that the 'wall effect' influences the velocity profile in the capillary for only about one-third of the length of its radius R ($R = 50$ μm).

In Fig. 8, the average velocity, $\langle v_{xp,c} \rangle_{w=p}$, of the liquid in a charged cylindrical capillary packed with charged particles versus the applied electric field E_x is presented, for different values of the diameter, d_p, of the particles and for two different values of the conductivity factor χ. The results clearly show that the value of the average velocity, $\langle v_{xp,c} \rangle_{w=p}$, of the EOF increases with increasing values of E_x and χ, and the increase in the value of $\langle v_{xp,c} \rangle_{w=p}$ with increasing values of E_x is linear. Furthermore, the results indicate that the effect of the particle diameter, d_p, on the value of the velocity of the EOF is very small; for all given values of E_x and χ, (i) the velocity $\langle v_{xp,c} \rangle_{w=p}$ when $d_p = 1.0$ μm, is only 1.67% larger than the value of the velocity when $d_p = 0.5$ μm, (ii) the value of the velocity when $d_p = 3.0$ μm, is only 1.10% larger than the value of the velocity when $d_p = 1.0$ μm, (iii) the value of $\langle v_{xp,c} \rangle_{w=p}$ when $d_p = 5.0$ μm, is only 0.22% larger than the value of the velocity when $d_p = 3.0$ μm, and (iv) the value of the velocity when $d_p = 10$ μm, is only 0.17% larger than the value of the velocity when $d_p = 5.0$ μm. Thus, because of these observations and since the value of the velocity when $d_p = 10$ μm is only 3.19% larger than the value of the velocity when $d_p = 0.5$ μm, and the value of $\langle v_{xp,c} \rangle_{w=p}$ when $d_p = 3.0$ μm is only 2.80% larger than the value of the velocity when $d_p = 0.5$ μm, for given values of E_x and χ, one could practically consider that the value of the average velocity, $\langle v_{xp,c} \rangle_{w=p}$, is almost independent of the particle diameter, d_p. This theoretical finding is in good agreement with the experimental results measured by different research groups [9,36]. In Fig. 9, the average velocity $\langle v_{xp,c} \rangle_{w=p}$ versus the particle diameter, d_p, is plotted for different values of the applied electric field, E_x. The results in Fig. 9 clearly

indicate the very weak dependence of $\langle v_{xp,c}\rangle_{w=p}$ on the particle diameter, d_p, since the lines are almost horizontal. The reason for this result is that the magnitudes of the radii, R_{ic}, of the interstitial channels for bulk flow in the packed capillary column, are such that the ratio R_{ic}/λ varies from 56.00 to 1120.07 (the ratio $R_{ic}/\lambda=56.00$ corresponds to the interstitial channels formed by the particles of diameter of 0.5 μm, while the ratio $R_{ic}/\lambda=1120.07$ corresponds to the interstitial channels formed by the particles of diameter of 10 μm) and, thus, for these ratios of R_{ic}/λ ($R_{ic}/\lambda=56.00$ is larger than the value of $R_{ic}/\lambda=50$ that was observed to provide an average velocity that was insignificantly different than the average velocities obtained when $R_{ic}/\lambda>50$) the average velocity of the EOF in the packed capillary column would change insignificantly with particle diameter.

In Fig. 10, the average velocity, $\langle v_{xp,c}\rangle_{w\neq p}$, of the EOF in a packed capillary column versus the diameter of the charged particles, d_p, is presented when the zeta potential at the wall, ζ_w, is different than the zeta potential, ζ_p, of the particles; the value of the conductivity factor χ is equal to 0.707 and the results are presented for four different values of the applied electric field, E_x. The results in Fig. 10 indicate that when $\zeta_w>\zeta_p$ the average velocity increases moderately as the particle diameter, d_p, increases, because there is a higher level of synergism between the velocity field due to the zeta potential of the wall and the velocity fields in the interstitial channels for bulk flow located close to the capillary wall since the diameters of such interstitial channels are larger when the particles have a larger diameter. When the value of ζ_p is 1.5 times larger than the value of ζ_w, there is a very slight increase in the value of the average velocity for values of d_p between 0.5 μm and about 1.5 μm (within this particle diameter range the velocity field is dominated by the zeta potential of the particles and the 'wall effect' due to ζ_w has insignificant influence); in fact, the system behavior when $\zeta_p=1.5\zeta_w$ and the particle diameter range is 0.5–1.5 μm, is similar to that exhibited in Fig. 9. Furthermore, one can observe that when $\zeta_p=1.5\zeta_w$ and the particle diameter increases above 1.5 μm, the average velocity of the EOF decreases slightly with increasing values of the particle diameter. This occurs because the slower velocity field due to the zeta potential of the wall starts having a more appreciable hindering effect on the velocity fields in the interstitial channels for bulk flow located close to the capillary wall, as the particle diameter increases above 1.5 μm and the diameters of these interstitial channels increase. In Fig. 10, it can also be observed that when $\zeta_w=1.0\times10^{-25}\zeta_p\cong0$, which would imply that the wall of the capillary column is uncharged, the results show that there is a decrease in the value of the average velocity, $\langle v_{xp,c}\rangle_{w\neq p}$, as the particle diameter, d_p, increases, and the magnitude of the decrease in the value of the average velocity increases as the magnitude of the applied electric field, E_x, increases. As the particle diameter, d_p, increases, the larger relatively dead volume close to the wall of the capillary column increases, and this larger dead volume decreases the velocity.

3.4. Comparisons between experimental and theoretical results

In Fig. 11, the theoretical results obtained from the model presented in this work for the determination of the average velocity, $\langle v_{xp,c}\rangle_{w=p}$, of the EOF in a capillary column packed with charged porous particles are compared with the experimental data measured (K.K. Unger, private communication, 1999) by Lüdtke [36]. The value of the conductivity factor, χ, that was found to provide the best fit between the experimental data and the theoretical values, is 0.716. The charged particles used in the experiments are porous silica C_8 particles whose zeta potential, ζ_p, at their surface was measured and found to be equal to -64.1 mV in the mobile liquid solution indicated in the figure caption. The charged porous particles were packed in a fused-silica capillary of radius $R=50$ μm and length $L=8.5$ cm, and the system was such that $\zeta_w\cong\zeta_p=-64.1$ mV; the value of the parameter ε_b was equal to 0.35. The pore size distribution of these particles [8,36] indicates that the pore radii are large enough that the theoretical results in Fig. 2a,b of this work would indicate that the velocity of the EOF could be greater than zero in a substantial fraction of the pores in the particles. The occurrence of intraparticle EOF could affect the value of the conductivity factor, χ [12,13,16,17,34], and since the value of $\chi=0.716$

provides the best fit with the experimental data and is slightly higher than the value of $\chi = 0.707$ suggested [35] for columns packed with impermeable spherical particles, one might infer, by considering also the results for the values of $\langle v_x \rangle$ in Fig. 2a,b, that the value of the velocity of the intraparticle EOF might be nonzero in the porous particles of the system in Fig. 11; the pore network modeling theory of Meyers and Liapis [12,13] could be used to determine the magnitude of the intraparticle velocity of the EOF in a future investigation. The results in Fig. 11 indicate that the agreement between theory and experiment is good.

In Fig. 12, the experimental values of the average velocity of the EOF in a capillary column packed with charged porous particles having a diameter, d_p, of 0.2 μm are presented, for different values of E_x and for three different values of the concentration, C_∞, of the electrolyte [36]. The charged particles used in the experiments [36] are porous silica C_8 particles which were packed in a fused-silica capillary of radius $R = 50$ μm and length $L = 8.5$ cm. The effect of the concentration, C_∞, of the electrolyte was studied by experiments performed [36] at three different values of C_∞ ($C_\infty = 5.0$ mM; $C_\infty = 10.0$ mM; $C_\infty = 25.0$ mM). The mobile liquid phase is 80% acetonitrile–20% C_∞ Tris–HCl (80:20, v/v) at pH 8.0 and temperature $T = 20$°C. The void fraction, ε_b, in the bed was equal to about 0.35 and the magnitude of the radius, R_{ic}, of the interstitial channels for bulk flow by EOF in the fused-silica capillary packed with silica C_8 particles whose radius, r_p, is 0.1 μm ($d_p = 2r_p = 0.2$ μm), is about one-third of the particle radius and, thus, $R_{ic} \cong 0.033$ μm which corresponds to 333.33 Å. The experimental data presented in Fig. 12 were obtained [36] by employing the same packed capillary column and, therefore, the value of the conductivity factor, χ, in Eq. (36) is taken to be the same in the theoretical calculations for all three values of C_∞. The theoretical predictions were compared with the experimental data and, for a given concentration of the electrolyte, C_∞, the best fit is obtained by finding the value of the zeta potential, ζ_p, at the surface of the particles that fits best the experimental data for the given value of C_∞ together with the value of the conductivity factor, χ, that was found to fit best the experimental data for all three different values of C_∞. In Fig. 12, the value of χ and the values of ζ_p that provide the best fit of the experimental data for the three different values of the concentration, C_∞, of the electrolyte, are presented. By examining the experimental data in Fig. 12 obtained by (S. Lüdtke, private communication, 1999; K.K. Unger, private communication, 1999) [36], one can observe that the majority of the experimental points for the systems where $C_\infty = 10.0$ mM and $C_\infty = 25.0$ mM could be described by lines that pass through the origin, as should be the case since $\langle v_{xp,c} \rangle_{w=p} = 0$ when $E_x = 0$. The experimental points for the system where $C_\infty = 5.0$ mM indicate that the data obtained at the higher values of E_x could be described by a line that passes through the origin, while some of the experimental data obtained at the lower values of E_x appear not to be described sufficiently accurately by the line that passes through the origin; this would suggest that the experimental accuracy of these points measured at the lower values of E_x may not be so good as for the other points. Lüdtke [36], Lüdtke (private communication, 1999) and Unger (private communication, 1999) have indicated that they are aware that their experimental measurements may not only reflect the velocity of the EOF in the packed capillary column but they might contain contributions by the frits and the unpacked part of the capillary column. Even though there may be certain inaccuracies in their experimental data, the agreement between theory and experiment is very gratifying. The results in Fig. 11 showed that the agreement between theory and experiments involving fused-silica capillaries packed with charged porous particles whose diameters ranged from 0.5 to 3.0 μm, was good. That agreement together with the agreement shown in Fig. 12, provide significant evidence for the capability of the theoretical model presented in this work to describe the velocity field of the EOF in CEC systems.

It is important to mention here that the values of the zeta potential, ζ_p, shown in Fig. 12 are very comparable to the value of -64.1 mV which represents the magnitude of the zeta potential, ζ_p, measured experimentally [36] at the surface of charged porous silica C_8 particles of diameter 0.5 μm in a mobile liquid phase of 80% acetonitrile–20% 25 mM Tris–HCl (80:20, v/v) at pH 8.0 and $T = 20$°C. In

fact, the value of $\zeta_p = -65.6$ mV determined from the best fit between the theoretical and the experimental results is only 2.34% larger than the experimentally measured value of $\zeta_p = -64.1$ mV at the same electrolyte concentration of $C_\infty = 25.0$ m*M*; this result is also very gratifying if one considers that the experimentally measured [36] value of ζ_p was with particles of 0.5 μm in diameter while the particles of the system in Fig. 12 have a diameter of 0.2 μm. Furthermore, the value of $\chi = 0.709$ in Fig. 12 compares very favorably with the value of $\chi = 0.716$ obtained for the results presented in Fig. 11.

3.5. Simulations describing the velocity of the EOF in packed capillaries for a wide range of operating conditions

In Figs. 13–18 the results of model simulations are presented for different CEC systems. The values of the parameters are reported in the text of this section and in the figures, the concentration, C_∞, of the symmetric electrolyte is 25 m*M*, $T = 20$°C, the radius, *R*, of the capillary column is 50 μm, and the length, *L*, is 8.5 cm; the bed porosity ε_b is 0.35, and the value of R_{ic} is taken to be equal to $(1/3)r_p$. By examining the equations of the mathematical model presented in this work, one can observe that the average velocity of the EOF increases when (i) the values of ε and E_x increase, (ii) the values of μ and ζ_p decrease (the value of ζ_p becomes more negative), and (iii) the value of ζ_w is more negative than the value of ζ_p. In Fig. 13, the average velocity, $\langle v_{xp,c} \rangle_{w=p}$, of the EOF in the capillary column packed with charged porous particles of diameter $d_p = 1.0$ μm is plotted versus the viscosity, μ, and the dielectric constant, ε, of the mobile liquid phase when (a) $E_x = 60$ kV/m, and (b) $E_x = 120$ kV/m; the value of ζ_p is equal to -64.1 mV, the value of ζ_w is equal to the value of ζ_p ($\zeta_w = \zeta_p$), and the magnitude of the conductivity factor, χ, is equal to 0.716. The results in Fig. 13 indicate that the value of $\langle v_{xp,c} \rangle_{w=p}$ increases as μ decreases and ε and E_x increase, and furthermore, the data show that while the magnitude of $\langle v_{xp,c} \rangle_{w=p}$ varies non-linearly as the values of μ and ε change, the value of the average velocity of the EOF depends more strongly on the magnitude of the viscosity, μ, than the value of the dielectric constant, ε. The results also indicate that the average velocity of the EOF can be doubled when the value of the applied electric field, E_x, increases by 100%. In Fig. 14, the average velocity of the EOF is plotted versus μ and ε when the capillary column is packed with charged porous particles of diameter $d_p = 3.0$ μm. The value of ζ_p is equal to -64.1 mV, $\zeta_w = \zeta_p$, $\chi = 0.716$, and two different values of E_x are examined; (a) $E_x = 60$ kV/m, and (b) $E_x = 120$ kV/m. By comparing the results in Figs. 13 and 14 it can be observed that for a given set of values of μ, ε, and E_x, the magnitude of the average velocity of the EOF is essentially unaffected by the value of the particle diameter, d_p; this occurs because the values of the ratio R_{ic}/λ for the systems in Figs. 13 and 14 are larger than 50 and the results of this work have shown that when $R_{ic}/\lambda \geq 50$ the average velocity of the EOF in the packed capillary column would change insignificantly with particle diameter. In Fig. 15, the average velocity of the EOF is plotted versus the zeta potential, ζ_p, at the surface of the particles and the applied electric field per unit length, E_x, when the diameter, d_p, of the charged porous particles packed in the capillary column is (a) 1.0 μm, and (b) 3.0 μm; the mobile liquid phase is 80% acetonitrile–20% 25 m*M* Tris–HCl (80:20, v/v), $\mu = 4.99 \times 10^{-4}$ Pa·s, $\varepsilon = 47.8$ esu^2/dyne per cm^2 (4.2288×10^{-10} C^2/N per m^2), $\zeta_w = \zeta_p$, and the value of the conductivity factor, χ, is 0.716. The results in Fig. 15 clearly indicate that both ζ_p and E_x affect significantly the value of $\langle v_{xp,c} \rangle_{w=p}$ and it can be observed that the magnitude of the average velocity of the EOF increases as E_x increases and ζ_p becomes more negative. Furthermore, by comparing the results in Fig. 15a,b one can observe that the magnitude of $\langle v_{xp,c} \rangle_{w=p}$ is virtually unaffected by the value of the particle diameter, d_p, because of the reason discussed above. Thus, the results in Figs. 13–15 indicate that for a given operationally permissible value of E_x, high values for the average velocity of the EOF can be obtained if (a) the zeta potential, ζ_p, at the surface of the particles packed in the column has a large negative magnitude, (b) the value of the viscosity, μ, of the mobile liquid phase is low, (c) the magnitude of the dielectric constant, ε, of the mobile liquid phase is reasonably large, and

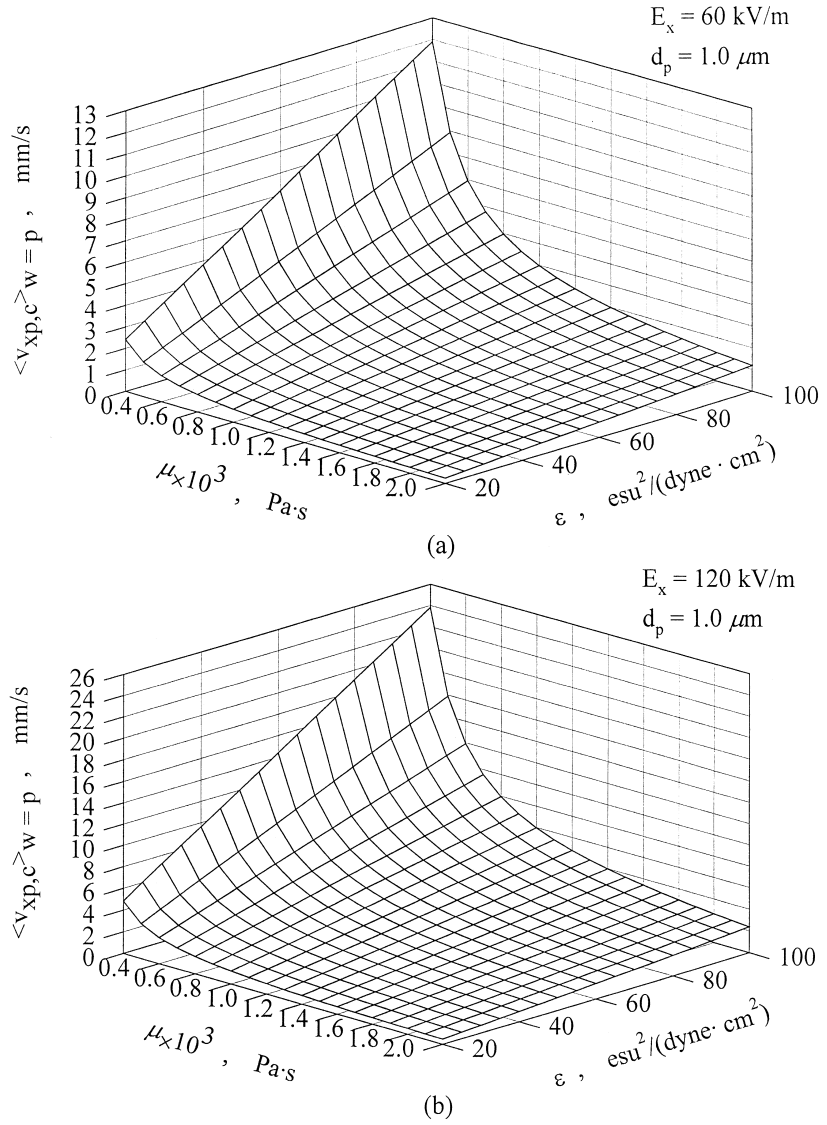

Fig. 13. Average velocity, $\langle v_{xp,c}\rangle_{w=p}$, of the EOF in a cylindrical capillary column of radius $R=50$ μm packed with charged particles of diameter $d_p=1.0$ μm for different values of the viscosity, μ, and dielectric constant, ε, and for two different values of the applied electric potential difference per unit length, E_x. The concentration of the symmetric electrolyte is $C_\infty=25$ mM; $\zeta_w=\zeta_p=-64.1$ mV; $\Phi(r=R)=\zeta_w$; and $T=20$°C. (a) $E_x=60$ kV/m, and (b) $E_x=120$ kV/m.

(d) the combination of the values of ε and C_∞ provide a thin double layer (Eq. (17)).

3.6. Estimates for the intraparticle velocity of the EOF and intraparticle Peclet number

In Fig. 16, the value of the intraparticle velocity, $v_{p,i}$, of the EOF of the liquid phase is plotted versus the tortuosity factor, τ, for different values of the mean pore radius, R_{pore}. The parameter R_{pore} represents the value of the mean radius of the pores in the charged porous particles and is determined from the pore size distribution [8,11–14,37] of the pores in the particles (intraparticle pores). The tortuosity

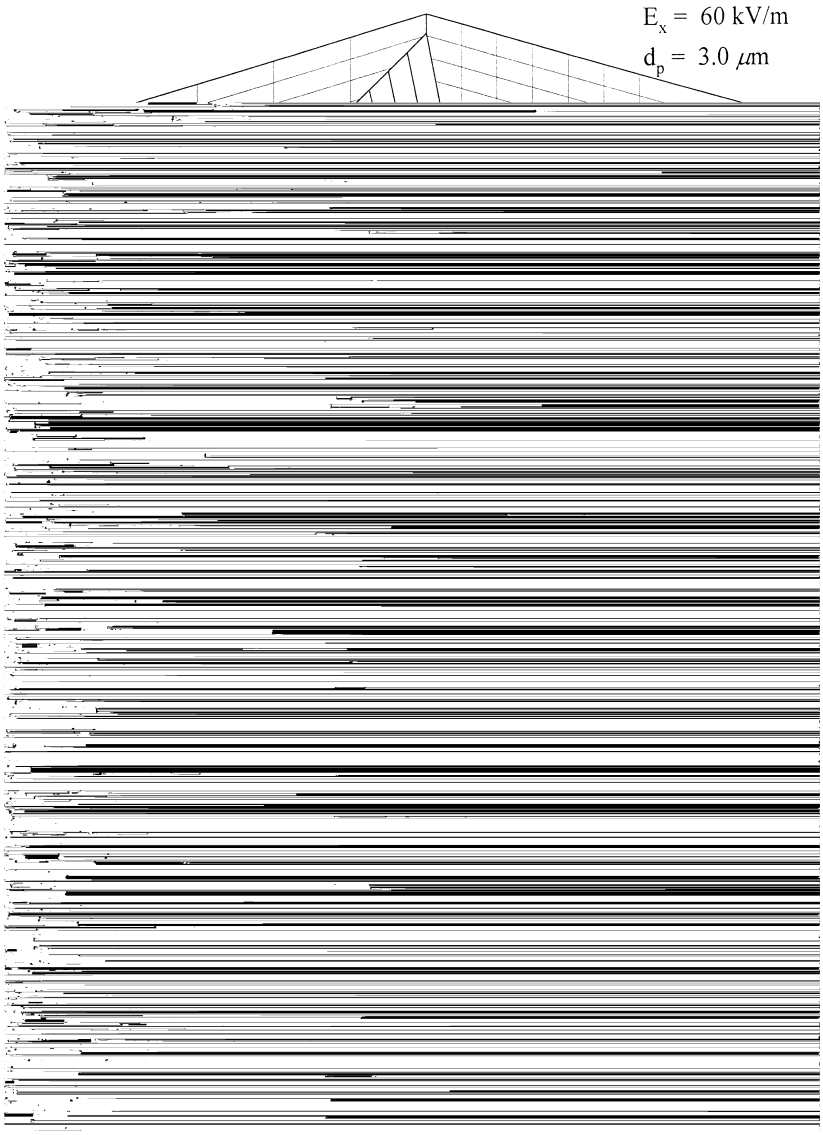

Fig. 14. Average velocity, $\langle v_{xp,c}\rangle_{w=p}$, of the EOF in a cylindrical capillary column of radius $R=50$ μm packed with charged particles of diameter $d_p=3.0$ μm for different values of the viscosity, μ, and dielectric constant, ε, and for two different values of the applied electric potential difference per unit length, E_x. The concentration of the symmetric electrolyte is $C_\infty=25$ mM; $\zeta_w=\zeta_p=-64.1$ mV; $\Phi(r=R)=\zeta_w$; and $T=20$°C. (a) $E_x=60$ kV/m, and (b) $E_x=120$ kV/m.

factor represents the ratio of the length of the tortuous pathway for mass transfer in the porous particles to the straight length pathway and, thus, in practice τ is greater than one ($\tau>1$). The intraparticle velocity, $v_{p,i}$, is given by:

$$v_{p,i}=\langle v_x\rangle\chi_1 \tag{39}$$

where $\langle v_x\rangle$ represents the average velocity of the EOF in a charged cylindrical pore (capillary) whose radius R is taken to be equal to the mean pore radius,

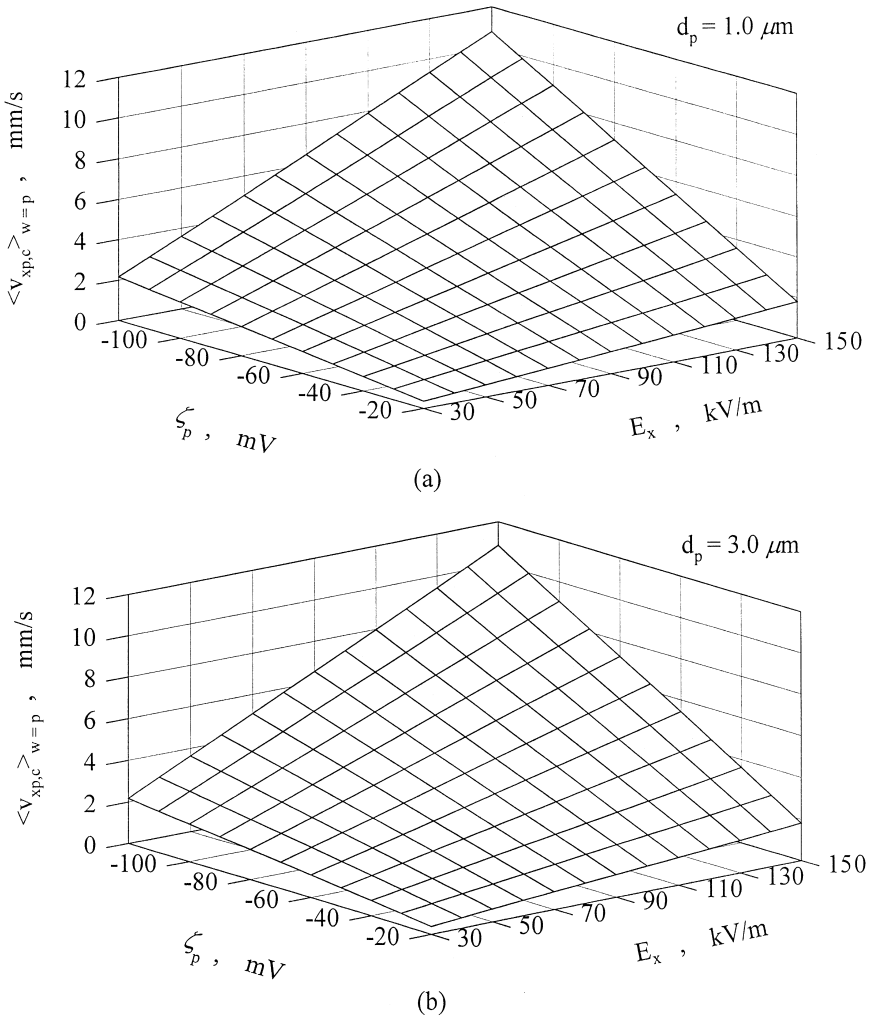

Fig. 15. Average velocity, $\langle v_{xp,c}\rangle_{w=p}$, of the EOF in a cylindrical capillary column of radius $R=50$ μm packed with charged particles for different values of the zeta potential, ζ_p, at the surface of the particles and of the applied electric potential difference per unit length, E_x, and for two different values of the particle diameter, d_p. The liquid solution is 80% acetonitrile–20% 25 m*M* Tris–HCl (80:20, v/v); $\zeta_w=\zeta_p$; $\Phi(r=R)=\zeta_w$; and $T=20$°C. (a) $d_p=1.0$ μm, and (b) $d_p=3.0$ μm.

R_{pore}, of the intraparticle pores ($R=R_{pore}$), and χ_1 denotes the conductivity factor which is given by the ratio of the effective conductivity of the charged porous particle when its pores are filled with the electrolyte solution to the conductivity when the porosity, ε_p, of the particle approaches unity and the pore volume that now approaches the particle volume is filled with the electrolyte solution. Accurate values for the conductivity χ_1 in Eq. (39) could be determined, for a given CEC system of interest, by using the pore network theory of Meyers and Liapis [12,13]. As a first approximation one may consider that the value of χ_1 could be estimated by the inverse of the tortuosity factor ($1/\tau$). It is worth noting that porous particles of practical significance are those whose porous structures provide continuous conducting pathways for mass transfer [12,13,37]; in this work, porous particles are considered whose porous structure has a pore size distribution and pore connectivity that do not allow a percolation threshold

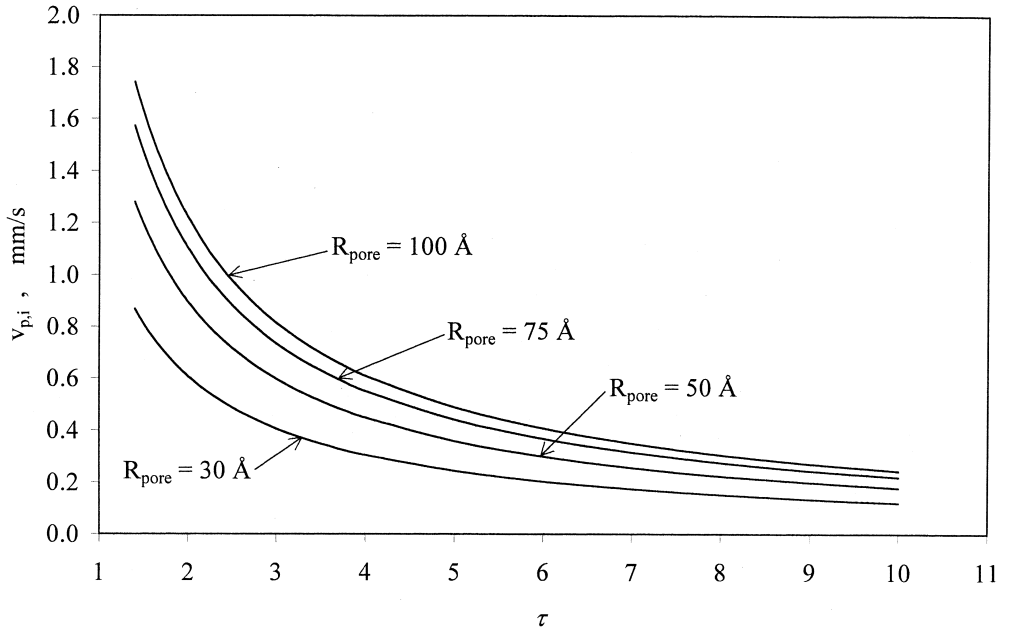

Fig. 16. Average intraparticle velocity, $v_{p,i}$, of the EOF in charged porous particles for different values of the tortuosity factor, τ, and of the mean pore radius, R_{pore}, determined from the pore size distribution of particles having different porous structures. The liquid solution is 80% acetonitrile–20% 25 m*M* Tris–HCl (80:20, v/v); the zeta potential, ζ_w, at the wall (surface) of the pore of radius R_{pore} is taken to be equal to the value of the zeta potential, ζ_p, at the surface of the particles, and $\Phi(r=R_{pore})=\zeta_w=\zeta_p=-64.1$ mV; pH 8.0; $T=20$°C; and $E_x=60$ kV/m.

to occur [12,13,37] and, thus, there are continuous conducting pathways for mass transfer in the porous structure of the particles. The value of the average velocity, $\langle v_x \rangle$, of the EOF in the charged cylindrical pore of radius R_{pore} is determined from Eq. (40):

$$\langle v_x \rangle = \frac{\int_0^{2\pi}\int_0^{R_{pore}} v_x r \, dr \, d\theta}{\pi R_{pore}^2} = \left(\frac{2}{R_{pore}^2}\right)\left(\int_0^{R_{pore}} v_x r \, dr\right) \quad (40)$$

In Eq. (40) the local velocity, v_x, is determined from the numerical solution of Eqs. (15), (18), (20), (21), (23), and (24) by replacing R by R_{pore}. The zeta potential, ζ_w, at the surface (wall) of the pores of the charged porous particle was taken to be approximately equal to the zeta potential, ζ_p, at the surface of the particles and for the data shown in Fig. 16 it was considered that $\Phi(r=R_{pore})=\zeta_w \cong \zeta_p=-64.1$ mV. The results in Fig. 16 clearly show that the value of the intraparticle velocity, $v_{p,i}$, is non-zero even when $R_{pore}=30$ Å and $\tau=10$; furthermore, as expected, the value of the intraparticle velocity, $v_{p,i}$, increases as R_{pore} increases and τ decreases. The findings in Fig. 16 are very important because they indicate that mass transfer in the pores of the charged porous particles employed in CEC could occur by intraparticle EOF since the magnitude of $v_{p,i}$ is greater than zero. Liapis et al. [15], Heeter and Liapis [16,38], and Xu and Liapis [18] have shown that (i) the isoconcentration profiles of the adsorbate molecules in spherical porous particles exhibit spherical symmetry when the value of the intraparticle velocity, $v_{p,i}$, is equal to zero (purely diffusive particles), and (ii) there is a departure from spherical symmetry of the isoconcentration profiles of the adsorbate molecules in spherical porous particles when the magnitude of the intraparticle velocity, $v_{p,i}$, is greater than zero (the isoconcentration profiles exhibit a spherical asymmetry when $v_{p,i}>0$). This spherical

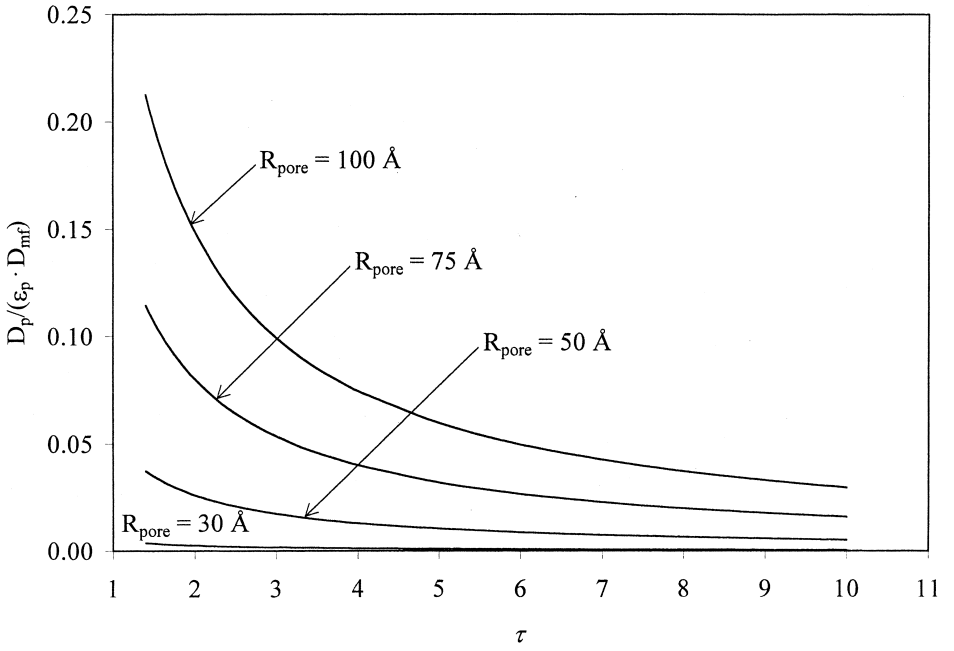

Fig. 17. Ratio of the effective pore diffusion coefficient, D_p, of the solute to $\varepsilon_p D_{mf}$ for different values of the tortuosity factor, τ, and of the mean pore radius, R_{pore}, determined from the pore size distribution of particles having different porous structures; $\varepsilon_p = 0.49$ and $D_{mf} = 1.006 \times 10^{-10}$ m^2/s.

asymmetry increases the adsorbate availability in the pore fluid and also increases the concentration of the adsorbate in the adsorbed phase in the upstream half of the spherical porous adsorbent particles; as the value of the intraparticle velocity, $v_{p,i}$, increases and the adsorbate concentration minimum moves downstream, the overall adsorbate content of the spherical adsorbent particles increases and, thus, the dynamic utilization of the adsorptive capacity of the column increases [15,16,18,38]. The technique of confocal microscopy [39,40] and the direct measurement method of Gustavsson et al. [41] could represent two possible methods for the experimental detection of the intraparticle velocity, $v_{p,i}$, of the EOF. In HPLC systems where the mobile liquid phase is driven by a pressure difference across the length of the packed column, intraparticle convective flow could occur when perfusive or gigaporous [12–18,38,41–47] particles are employed. The gigaporous particles provide faster intraparticle mass transfer rates than the conventional porous particles at the expense of having lower capacities than the conventional porous particles, because the latter have larger internal surface areas per unit volume of the particle than the gigaporous particles. Therefore, the results in Fig. 16 indicate that CEC systems employing conventional porous particles could provide fast intraparticle mass transfer rates because the intraparticle velocity of the EOF (the intraparticle convective flow due to EOF) could be greater than zero, as well as high capacities. Furthermore, it appears that if the appropriate diameter, d_p, for the charged porous particles is selected for the packed bed, the mobile liquid phase could be driven through the packed bed by the simultaneous application of pressure and electric potential differences across the length of the column (hybrid system); such a hybrid operational strategy would increase the velocity of the fluid in the interstitial channels for bulk flow in the packed bed and would also provide fast intraparticle mass transfer rates. It should be noted that the pore network theory of Meyers and Liapis [12,13] could be used to obtain

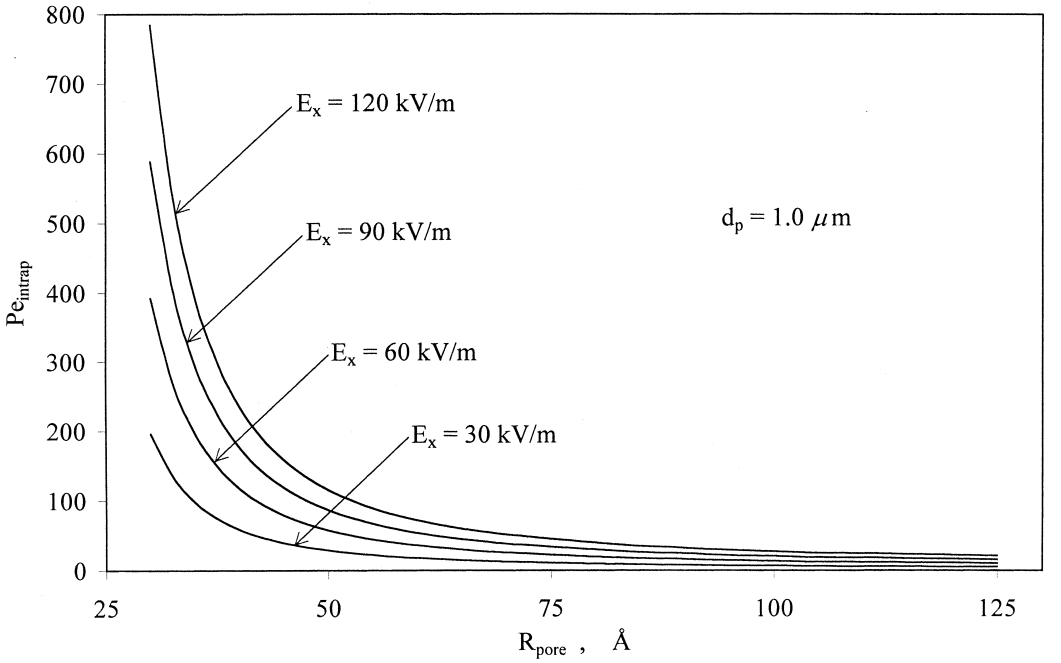

Fig. 18. Intraparticle Peclet number, $Pe_{int\ rap}$, of the solute versus the mean pore radius, R_{pore}, determined from the pore size distribution of particles having different porous structures, for various values of the applied electric potential difference per unit length, E_x; the diameter, d_p, of the particles is equal to 1.0 μm. The liquid solution is 80% acetonitrile–20% 25 m*M* Tris–HCl (80:20, v/v); the zeta potential, ζ_w, at the wall (surface) of the pore of radius R_{pore} is taken to be equal to the value of the zeta potential, ζ_p, at the surface of the particles, and $\Phi(r=R_{pore})=\zeta_w=\zeta_p=-64.1$ mV; pH 8.0; and $T=20$°C.

more accurate values for the intraparticle velocity, $v_{p,i}$, of the EOF.

The value of δ that would correspond to a zeta potential, ζ_w, value of −64.1 mV at the wall of charged cylindrical capillaries whose radii are such that $R/\lambda \geq 50$ (R denotes the radius of the charged cylindrical capillary), is equal to −7004.94 esu/cm^2. The mean pore radii considered in Fig. 16 provide values of R_{pore}/λ (R is replaced by the radius, R_{pore}, of the pore) that vary between 2.02 and 6.72. In Table 1, the values of the average velocity, $\langle v_x \rangle$, are presented for different values of the mean pore radius, R_{pore}, when the value of δ at the wall of the pore is kept constant and equal to −7004.94 esu/cm^2. Also in Table 1 the values of $\langle v_x \rangle$ when the value of ζ_w is kept constant and equal to −64.1 mV are presented, for various values of the mean pore radius, R_{pore}; these values of $\langle v_x \rangle$ were used in Eq. (39) to obtain the values of $v_{p,i}$ reported in Fig. 16. By comparing the values of $\langle v_x \rangle$ in Table 1, it can be observed that the intraparticle velocity of the EOF is slightly higher when the value of δ is kept constant; the differences become very small as the value of the mean pore radius, R_{pore}, increases and the ratio R_{pore}/λ increases, for the reasons discussed above (the largest difference is 16.92% when $R_{pore}=30$ Å and the smallest difference is 3.33% when $R_{pore}=100$ Å).

In Fig. 17, the ratio of the effective pore diffusion coefficient, D_p, of lysozyme to the product of the particle porosity, ε_p, with the free molecular diffusion coefficient, D_{mf}, of lysozyme is plotted versus the tortuosity factor, τ, for different values of the mean pore radius, R_{pore}. The effective pore diffusion coefficient, D_p, of lysozyme was estimated [12,13,47] from the expression:

Table 1
Values of the average velocity, $\langle v_x \rangle$ (Eq. (40)), in cylindrical capillaries of varying mean pore radii, R_{pore}, for the case where the value of the zeta potential, ζ_p, at the wall of the pores is kept constant and equal to −64.1 mV and for the case where the fixed charge density, δ, at the wall of the pores is kept constant and equal to −7004.94 esu/cm^2[a]

Mean pore radius, R_{pore} (Å)	R_{pore}/λ	Case where $\zeta_p = -64.1$ mV for all values of R_{pore}	Case where $\delta = -7004.94$ esu/cm^2 for all values of R_{pore}
		$\langle v_x \rangle$ (mm/s)	$\langle v_x \rangle$ (mm/s)
30	2.02	1.217	1.423
50	3.36	1.791	1.936
75	5.04	2.203	2.308
100	6.72	2.441	2.522

[a] The mobile liquid phase is 80% acetonitrile–20% 25 m*M* Tris–HCl (80:20, v/v), pH 8.0, $T = 20$°C, $\lambda = 14.88$ Å, and $E_x = 60$ kV/m.

$$D_p = \frac{(\varepsilon_p D_{mf})\beta}{\tau} \quad (41)$$

where β represents the hindrance parameter that accounts for hindered diffusion and steric effects [12,13,37,48–53]; β is a function of the effective molecular radius, α_1, of the diffusing solute and of the pore size, R_{pore}, and can usually be determined with reasonable accuracy [47,50]. The value of the porosity, ε_p, of the particle was taken to be equal to 0.49 [8], and the values of the effective molecular radius, α_1, and of the free molecular diffusion coefficient, D_{mf}, of lysozyme were taken to be [12] 21.4 Å and 1.006×10^{-10} m^2/s, respectively. The values of β obtained from the theoretical predictions of Brenner and Gaydos [50] for the different values of R_{pore} considered in Fig. 17, are as follows: $\beta = 5.245 \times 10^{-3}$ when $R_{pore} = 30$ Å; $\beta = 5.241 \times 10^{-2}$ when $R_{pore} = 50$ Å; $\beta = 0.160$ when $R_{pore} = 75$ Å; $\beta = 0.298$ when $R_{pore} = 100$ Å. The results in Fig. 17 clearly indicate that the value of the ratio $D_p/\varepsilon_p D_{mf}$ increases as the size of the mean pore radius, R_{pore}, increases and the value of the tortuosity factor, τ, decreases. If the diffusion pathways are not tortuous and if there are no hindered diffusion and steric effects, then the hypothetical maximum value of D_p would be equal to $\varepsilon_p D_{mf}$, and this would imply from Eq. (41) that the maximum value of the ratios $D_p/\varepsilon_p D_{mf}$ and β/τ (because $D_p/\varepsilon_p D_{mf} = \beta/\tau$ from Eq. (41)) would be equal to one. Meyers and Liapis [12,13] by determining and employing the pore size distribution and pore connectivity of the porous structure of the particles in their pore network theory, can determine in an a priori manner the value of the effective pore diffusion coefficient, D_p, of a solute of interest under unretained and under retained conditions, and therefore, their theory can determine in an a priori manner the value of the ratio $D_p/\varepsilon_p D_{mf}$. Their results [12,13] clearly show that the value of the ratio $D_p/\varepsilon_p D_{mf}$ increases as the pore connectivity of the porous structure of the particles increases. The results in Fig. 17 and in the work of Meyers and Liapis [12,13] indicate that in order to obtain high values of the effective pore diffusion coefficient, D_p, the size of the pores in the porous particles employed in CEC (and in HPLC) should be such that steric hindrance at the entrance to the pores and frictional resistance within the pores are small, and also the magnitude of the pore connectivity of the porous structure should be high so that it together with the appropriate pore size distribution could decrease significantly the effects of hindered diffusion and the length of the tortuous diffusion pathways in the porous structure of the particles.

In Fig. 18, the intraparticle Peclet number, $Pe_{int\ rap}$, for lysozyme is plotted versus the mean pore radius, R_{pore}, for different values of E_x and for particles whose diameter, d_p, is equal to 1.0 μm. The different values of E_x provide different values for the intraparticle velocity of the EOF. The intraparticle Peclet number, $Pe_{int\ rap}$, represents the ratio of the diffusional response time, t_d, to the convective (flow) response time, t_c, of a solute in a porous particle and, thus,

$$\mathrm{Pe}_{\mathrm{int\ rap}} = \frac{t_d}{t_c} \tag{42}$$

Under unretained conditions, t_d is the time required for diffusional equilibration of the solute in the porous medium with its surroundings and t_c is the time required to replace solute in the porous medium by flow. If $t_d > t_c$ then the intraparticle Peclet number is greater than unity. The magnitude of t_d could be estimated from expression (43):

$$t_d \cong \frac{r_p^2}{6D_p} = \frac{d_p^2}{24D_p} \tag{43}$$

while the magnitude of t_c could be estimated from Eq. (44):

$$t_c \cong \frac{r_p}{v_{p,i}} = \frac{d_p}{2v_{p,i}} \tag{44}$$

In Eq. (44), $v_{p,i}$ represents the intraparticle velocity and its value could be determined from Eq. (39). By combining Eqs. (42)–(44) the following expression for $\mathrm{Pe}_{\mathrm{int\ rap}}$ is obtained and used to provide the results in Fig. 18:

$$\mathrm{Pe}_{\mathrm{int\ rap}} = \frac{d_p v_{p,i}}{12D_p} \tag{45}$$

The results in Fig. 18 indicate that the value of $\mathrm{Pe}_{\mathrm{int\ rap}}$ increases as the magnitude of E_x increases (higher values of E_x provide higher values for the intraparticle velocity, $v_{p,i}$, of the EOF) and the value of the mean pore radius, R_{pore}, decreases (lower values of R_{pore} decrease the value of $v_{p,i}$ and of the effective pore diffusion coefficient, D_p, but the decrease in the value of D_p is larger than the decrease in the value of $v_{p,i}$). It is important to note that the value of the $\mathrm{Pe}_{\mathrm{int\ rap}}$ is greater than one even when $E_x = 30$ kV/m and $R_{pore} = 125$ Å. In fact, the values of $\mathrm{Pe}_{\mathrm{int\ rap}}$ when $R_{pore} = 125$ Å are as follows for the different values of E_x: $\mathrm{Pe}_{\mathrm{int\ rap}} = 5.3$ when $E_x = 30$ kV/m; $\mathrm{Pe}_{\mathrm{int\ rap}} = 10.6$ when $E_x = 60$ kV/m; $\mathrm{Pe}_{\mathrm{int\ rap}} = 15.9$ when $E_x = 90$ kV/m; $\mathrm{Pe}_{\mathrm{int\ rap}} = 21.3$ when $E_x = 120$ kV/m. Thus, the results in Fig. 18 indicate that $\mathrm{Pe}_{\mathrm{int\ rap}}$ is greater than one ($t_d > t_c$) for all values of R_{pore} and E_x considered. In CEC systems it would be desirable to obtain, for a given particle diameter, d_p, and an operationally acceptable value of the effective pore diffusion coefficient, D_p, high values for the intraparticle Peclet number, $\mathrm{Pe}_{\mathrm{int\ rap}}$, which means that it is desirable to operate at conditions that generate high values of the intraparticle velocity, $v_{p,i}$, of the EOF. It has been shown [15,16,18,38], as discussed earlier, that as the intraparticle velocity, $v_{p,i}$, increases and the value of $\mathrm{Pe}_{\mathrm{int\ rap}}$ increases, the concentrations of the solute in the pore fluid and in the adsorbed phase increase in the upstream half of the spherical porous adsorbent particles, the adsorbate concentration minimum moves downstream, the overall solute content of the porous particles increases and, thus, the dynamic utilization of the adsorptive capacity of the column increases. Therefore, as the intraparticle velocity, $v_{p,i}$, of the EOF increases, the intraparticle mass transfer resistance and the dispersive mass transfer effects decrease and, thus, higher column efficiency and resolution are obtained, if the appropriate chemistry is employed in the mobile liquid phase and in the charged porous particles of the CEC system of interest.

4. Conclusions

A mathematical model has been constructed and solved to describe quantitatively the profiles of the electrostatic potential, pressure, and velocity of the electroosmotic flow (EOF) in charged cylindrical capillaries and in capillary columns packed with charged particles. The results obtained from model simulations have (i) provided significant physical insight and understanding with regard to the velocity profile of the EOF in capillary columns packed with porous charged particles which represent systems employed in capillary electrochromatography (CEC), (ii) provided the physical explanation for the experimental results which indicate that the average velocity of the EOF in capillary columns packed with porous particles is a very weak function (it is almost independent) of the diameter of the particles, and (iii) indicated that the intraparticle velocity, $v_{p,i}$,

of the EOF can be greater than zero, because the magnitudes of the radii of the pores of the porous particles make the value of the ratio R_{pore}/λ (R_{pore} is the pore radius and λ is the characteristic length of the double layer) to be such that the average velocity of the EOF in a significant fraction of the pores in the particles could be greater than zero; thus, if the appropriate chemistry is employed in the mobile liquid phase and in the charged porous particles, the occurrence of intraparticle EOF could significantly reduce the mass transfer resistance in the porous particles. It was found that for an operationally acceptable value of the effective pore diffusion coefficient, D_p, of a solute, high values for the intraparticle Peclet number, $Pe_{int\ rap}$, could be obtained as higher values of E_x and R_{pore} generate intraparticle velocities of increasing magnitude. It has been shown [15,16,18,38] that as the value of $Pe_{int\ rap}$ increases, the concentration of the solute in the pore fluid and in the adsorbed phase increase in the upstream half of the spherical porous adsorbent particles, the adsorbate concentration minimum moves downstream, the overall solute content of the porous particles increases and, thus, the dynamic utilization of the adsorptive capacity of the column increases. Furthermore, the results from model simulations indicated that for a given operationally permissible value of the applied electric potential difference per unit length, E_x, high values for the average velocity of the EOF can be obtained if (a) the zeta potential, ζ_p, at the surface of the particles packed in the column has a large negative magnitude, (b) the value of the viscosity, μ, of the mobile liquid phase is low, (c) the magnitude of the dielectric constant, ε, of the mobile liquid phase is reasonably large, and (d) the combination of the values of the concentration, C_∞, of the electrolyte and of the dielectric constant, ε, provide a thin double layer.

The theoretical results for the velocity of the EOF obtained from the solution of the model presented in this work were compared with the experimental values of the velocity of the EOF obtained from a fused-silica column packed with charged porous silica C_8 particles. Systems with four different particle diameters and three different concentrations of the electrolyte were considered, and the magnitude of the applied electric field was varied widely. The agreement between theory and experiment was found to be good.

5. Nomenclature

C_+	concentration of positive ions (mol/m^3)
C_-	concentration of negative ions (mol/m^3)
$C_{+\infty}$	concentration of positive ions in the electroneutral core (mol/m^3)
$C_{-\infty}$	concentration of negative ions in the electroneutral core (mol/m^3)
C_∞	concentration of positive or negative ions in the electroneutral core for a symmetric electrolyte (mol/m^3)
CEC	capillary electrochromatography
D_{mf}	free molecular diffusion coefficient of solute (m^2/s)
D_p	effective pore diffusion coefficient of solute in the porous particle (m^2/s)
d_p	particle diameter ($d_p = 2r_p$) (m)
E_x	applied electric potential difference per unit length along the axial direction (kV/m)
e	charge on electron (1.60199×10^{-19} C)
EOF	electroosmotic flow
$\mathbf{F}_{drag}$	net drag force acting on an annular element (N)
$\mathbf{F}_{vis}$	net viscous force acting on an annular element (N)
I_0	zero order modified Bessel function of the first kind
i_x	axial current density (C/m^2 per s)
k	Boltzmann constant (1.38048×10^{-23} J/molecule per K)
L	length of cylindrical capillary (m)
N_o	Avogadro's number (6.023×10^{23} mol^{-1})
$n_{T,ic}$	connectivity of the interstitial channels of bulk flow
$n_{T,p}$	connectivity of the pores in the charged porous particles
P	pressure (N/m^2)
P_0	pressure at the centerline of the cylindrical capillary (N/m^2)
$Pe_{int\ rap}$	intraparticle Peclet number defined in

	Eq. (42) (see also Eq. (45)), dimensionless
R	radius of the cylindrical capillary (m)
R_{ic}	radius of the interstitial channels of bulk flow in a capillary column packed with charged particles (m)
R_{pore}	mean pore radius determined from the pore size distribution of the pores in the porous structure of the charged porous particle (m)
r	radial coordinate in a cylindrical capillary, or pore, or interstitial channel of bulk flow (m)
r_p	particle radius ($r_p = d_p/2$) (m)
T	temperature (K)
t_c	convective (intraparticle electroosmotic flow) response time (s)
t_d	diffusional response time (s)
$\mathbf{v}$	velocity vector (m/s)
$v_{p,i}$	intraparticle velocity of the electroosmotic flow (Eq. (39)) (m/s)
v_r	radial velocity component (m/s)
v_x	local axial velocity in a cylindrical capillary or pore (m/s)
$\langle v_x \rangle$	average axial velocity in a cylindrical capillary or pore (m/s)
$v_{x,max}$	maximum value of v_x in a cylindrical capillary when the value of R/λ permits a plug-flow profile to occur (m/s)
$v_{xp,c,w=p}$	velocity in a cylindrical capillary packed with charged particles when $\zeta_w = \zeta_p$ (m/s)
$\langle v_{xp,c} \rangle_{w=p}$	average velocity in a cylindrical capillary packed with charged particles when $\zeta_w = \zeta_p$ (m/s)
$v_{xp,c,w\neq p}$	velocity in a cylindrical capillary packed with charged particles when $\zeta_w \neq \zeta_p$ (m/s)
$\langle v_{xp,c} \rangle_{w\neq p}$	average velocity in a cylindrical capillary packed with charged particles when $\zeta_w \neq \zeta_p$ (m/s)
$v_{xp,un}$	velocity in a cylindrical capillary packed with uncharged (neutral) particles (m/s)
$\langle v_{xp,un} \rangle$	average velocity in a cylindrical capillary packed with uncharged (neutral) particles (m/s)
v_θ	angular velocity component (m/s)
x	axial coordinate in cylindrical capillary (m)
z_+	charge number of positive ions
z_-	charge number of negative ions
z	charge number of ions in symmetric electrolyte ($z = z_+ = -z_-$)

Greek letters

α_1	effective molecular radius of solute (m)
β	hindrance parameter that accounts for steric effects and hindered diffusion, dimensionless
$\Gamma(x)$	applied electric potential (Eq. (6)) (V)
γ	dimensionless packing parameter (Eq. (28))
δ	fixed charge density on the wall of a charged cylindrical capillary or pore (C/m^2)
ε	dielectric constant of the liquid solution (C^2/N per m^2)
ε_b	bed porosity in the capillary column (dimensionless)
ε_p	porosity of the charged porous particle (dimensionless)
ζ_p	zeta potential at the particle surface (V)
ζ_w	zeta potential at the capillary wall or at the surface (wall) of a pore (V)
θ	angular coordinate in cylindrical capillary (radians)
κ	dimensionless packing parameter defined in Eq. (31)
λ	Debye length parameter (Eq. (17)) (m)
μ	viscosity of liquid solution (kg/m per s)
ρ	density of liquid solution (kg/m^3)
ρ_{cd}	liquid solution space charge density (C/m^3)
τ	tortuosity factor (dimensionless)
Φ	electrostatic part of Ψ (Eq. (6)) (V)
Φ_1	$ez\Phi/kT$
$\Phi_{1,0}$	value of Φ_1 at the centerline of the cylindrical capillary
Φ_w	value of Φ at the capillary wall (V)
χ	conductivity factor defined below Eq. (35) (dimensionless)
χ_1	conductivity factor defined below Eq. (39) (dimensionless)
Ψ	total electrical potential (Eq. (6)) (V)

Subscripts

x	denotes the direction along the axis of the capillary column

Acknowledgements

The authors are grateful to Professor K.K. Unger and Dr S. Lüdtke of the Institut für Anorganische Chemie und Analytische Chemie of Johannes Gutenberg-Universität, Mainz, Germany, for helpful discussions and for the experimental measurements which appear in Figs. 11 and 12. Furthermore, we are grateful to Dr C. Bellmann and Mrs B. Gäbisch of the Institut für Polymerforschung, Dresden, Germany, for measuring the value of the zeta potential at the surface of the particles. The authors also acknowledge helpful discussions with Professors P. Neogi and O.K. Crosser of the Department of Chemical Engineering of the University of Missouri-Rolla. The authors also gratefully acknowledge support of this work by Criofarma and the Biochemical Processing Institute of the University of Missouri-Rolla.

References

[1] C.L. Rice, R. Whitehead, J. Phys. Chem. 69 (1965) 4017.
[2] V. Pretorius, B.J. Hopkins, J.D. Schieke, J. Chromatogr. 99 (1974) 23.
[3] W.-H. Koh, J.L. Anderson, AIChE J. 21 (1975) 1176.
[4] S. Levine, J.R. Marriott, K. Robinson, J. Chem. Soc. Faraday Trans. II 71 (1975) 1.
[5] J.H. Knox, I.H. Grant, Chromatographia 24 (1987) 135.
[6] S.S. Dukhin, Adv. Colloid Interface Sci. 35 (1991) 173.
[7] M.M. Dittmann, G.P. Rozing, G. Ross, T. Adam, K.K. Unger, J. Cap. Elec. 4 (1997) 201.
[8] S. Lüdtke, T. Adam, K.K. Unger, J. Chromatogr. A 786 (1997) 229.
[9] A.S. Rathore, Cs. Horvath, J. Chromatogr. A 781 (1997) 185.
[10] J.H. Knox, H.P. Scott, J. Chromatogr. 316 (1984) 311.
[11] F.A.L. Dullien, Porous Media: Fluid Transport and Pore Structure, 2nd Edition, Academic Press, New York, 1992.
[12] J.J. Meyers, A.I. Liapis, J. Chromatogr. A 827 (1998) 197.
[13] J.J. Meyers, A.I. Liapis, J. Chromatogr. A 852 (1999) 3.
[14] A.I. Liapis, Math. Model. Sci. Comput. 1 (1993) 397.
[15] A.I. Liapis, Y. Xu, O.K. Crosser, A. Tongta, J. Chromatogr. A 702 (1995) 45.
[16] G.A. Heeter, A.I. Liapis, J. Chromatogr. A 711 (1995) 3.
[17] G.A. Heeter, A.I. Liapis, J. Chromatogr. A 743 (1996) 3.
[18] Y. Xu, A.I. Liapis, J. Chromatogr. A 724 (1996) 13.
[19] E.N. da C. Andrade, C. Dodd, Proc. R. Soc. A204 (1951) 449.
[20] J.R. Melcher, G.I. Taylor, Electrohydrodynamics: a review of the role of interfacial shear stresses, in: W.R. Sears, M. van Dyke (Eds.), Annual Review of Fluid Mechanics, Vol. 1, Annual Review, Palo Alto, CA, 1969, pp. 111–146.
[21] A.J. Babchin, J. Colloid Interface Sci. 49 (1974) 390.
[22] S.S. Dukhin, N.A. Mishchuk, J. Membr. Sci. 79 (1993) 199.
[23] N.A. Mishchuk, P.V. Takhistov, Colloids Surf. A: Physicochem. Eng. Asp. 95 (1995) 119.
[24] R. Asiaie, X. Huang, D. Farnan, Cs. Horvath, J. Chromatogr. A 806 (1998) 251.
[25] J.C. Fair, J.F. Osterle, J. Chem. Phys. 54 (1971) 3307.
[26] J.C. Slattery, Momentum, Energy, and Mass Transfer in Continua, Robert E. Krieger Publishing, Huntington, NY, 1978.
[27] B.A. Grimes, Report No. 21, Department of Chemical Engineering, University of Missouri-Rolla, Rolla, MO, USA, 1999.
[28] W.B. Russel, D.A. Saville, W.R. Schowalter, Colloidal Dispersions, Cambrige University Press, Cambridge, UK, 1989.
[29] B.V. Zhmud, J. Colloid Interface Sci. 183 (1996) 111.
[30] J. Villadsen, M.L. Michelsen, Solution of Differential Equation Models by Polynomial Approximation, Prentice-Hall, Englewood Cliffs, NJ, 1978.
[31] C.D. Holland, A.I. Liapis, Computer Methods for Solving Dynamic Separation Problems, McGraw-Hill, New York, 1983.
[32] J. Happel, H. Brenner, Low Reynolds Number Hydrodynamics with Special Applications to Particulate Media, Prentice-Hall, Englewood Cliffs, NJ, 1965.
[33] R.F. Probstein, Physicochemical Hydrodynamics, Butterworth, Stoneham, MA, 1989.
[34] G. Neale, N. Epstein, W. Nader, Chem. Eng. Sci. 28 (1973) 1865.
[35] D.J. Gunn, Chem. Eng. Sci. 42 (1987) 363.
[36] S. Lüdtke, Ph.D. Dissertation, Institut für Anorganische Chemie und Analytische Chemie, Johannes Gutenberg-Universität, Mainz, Germany (1999).
[37] J.H. Petropoulos, A.I. Liapis, N.P. Kolliopoulos, J.K. Petrou, N.K. Kanellopoulos, Bioseparation 1 (1990) 69.
[38] G.A. Heeter, A.I. Liapis, J. Chromatogr. A 734 (1996) 105.
[39] A. Ljunglöf, J. Thömmes, J. Chromatogr. A 813 (1998) 387.
[40] A. Ljunglöf, P. Bergvall, R. Bhikhabhai, R. Hjorth, J. Chromatogr. A 844 (1999) 129.
[41] P.-E. Gustavsson, A. Axelsson, P.-O. Larsson, J. Chromatogr. A 795 (1998) 199.
[42] L. Lloyd, F.P. Warner, J. Chromatogr. 512 (1990) 365.
[43] N.B. Afeyan, S.P. Fulton, N.F. Gordon, I. Mazsaroff, L. Varady, F. Regnier, Bio/Technology 8 (1990) 203.
[44] N.B. Afeyan, N.F. Gordon, I. Mazsaroff, L. Varady, S.P. Fulton, Y.B. Yang, F. Regnier, J. Chromatogr. 519 (1990) 1.
[45] A.I. Liapis, M.A. McCoy, J. Chromatogr. 599 (1992) 87.
[46] K.-C. Loh, D.I.C. Wang, J. Chromatogr. A 718 (1995) 239.
[47] D.D. Frey, E. Schweinheim, Cs. Horvath, Biotechnol. Prog. 9 (1993) 273.

[48] E.M. Renkin, J. Gen. Physiol. 38 (1954) 225.
[49] K.H. Keller, T.R. Stein, Math. Biosci. 1 (1967) 421.
[50] H. Brenner, L.J. Gaydos, J. Colloid Interface Sci. 58 (1977) 312.
[51] E.A. Mason, R.P. Wendt, E.H. Bresler, J. Membr. Sci. 6 (1980) 283.
[52] H.J. Keh, PhysicoChem. Hydrodynamics 7 (1986) 281.
[53] W.M. Deen, AIChE J. 33 (1987) 1409.